CASE STUDY TO EVALUATE DRIFT ESTIMATION IN NON-DUCTILE REINFORCED CONCRETE BUILDINGS WITH FOUNDATION LAP-SPLICES: NUMERICAL SIMULATION WORK

by

Rebeca P. Orellana Montano

A Thesis

Submitted to the Faculty of Purdue University

In Partial Fulfillment of the Requirements for the degree of

Master of Science in Civil Engineering

Lyles School of Civil Engineering

West Lafayette, Indiana

August 2020

THE PURDUE UNIVERSITY GRADUATE SCHOOL
STATEMENT OF COMMITTEE APPROVAL

Dr. Julio A. Ramirez, Chair

Lyles School of Civil Engineering

Dr. Shirley J. Dyke

Lyles School of Civil Engineering and School of Mechanical Engineering

Dr. Ayhan Irfanoglu

Lyles School of Civil Engineering

Approved by:

Dr. Dulcy M. Abraham

Dedicated to my family and friends.

ACKNOWLEDGMENTS

I would like to thank my committee members Dr. Julio Ramirez, Dr. Ayhan Irfanoglu, and Dr. Shirley Dyke for supporting and guiding me throughout my graduate school journey. I especially wish to express my deepest gratitude to my advisor Dr. Ramirez for the continued support, invaluable insight, and encouragement. I am also thankful for having had the opportunity to do research and TA, instrumental in my learning interest and journey. The contributions of my advisor, committee members, and professors at Purdue University made possible the completion of this study.

Additionally, I would also like to thank my fellow classmates for the friendship and support during our time at Purdue. I am grateful for the connections made as a graduate student and the support of the department and faculty. A special thanks to my parents and siblings for always teaching me to believe in myself, to learn from challenges, and to pursue my dreams. The encouragement from loved ones, as I call my support system, has made me who I am today and I am extremely grateful and humble to have finished my graduate studies.

TABLE OF CONTENTS

LIST OF TABLES

LIST OF FIGURES

ABSTRACT

Past earthquake damage assessments have shown the seismic vulnerability of older non-ductile reinforced concrete buildings. The life safety-risk these buildings pose has motivated researchers to study, develop, and improve modeling techniques to better simulate their behavior with the aim to prioritize retrofits.

This study focuses on the lap splice detailing at the base of the building in columns, shorter than those recommended by modern codes which consider seismic effects. Current modeling efforts in non-ductile reinforced concrete frame structures have considered the connection at the foundation fixed. This study models the influence of the performance of short lap splices on the simulation of response of an instrumented perimeter-frame-non-ductile building located in Van Nuys, California, and to compare results with those of previous studies of the same building.

The methodology consisted of evaluating the response of a non-ductile concrete building subjected to a suite of ground motions through the comparison of three base connections: fixed, pinned, and a rotational spring modeling the short lap splice. Comparison and performance evaluation are done on the basis of drift as the main performance metric. In the building response evaluation flexure and shear forces in frame elements were also compared using the different base conditions.

The models consist of two-dimensional frames in orthogonal direction, including interior and exterior frames, totaling into 4 frames. The dynamic analysis was performed using SAP2000 analysis software. The proposed rotational spring at the base was defined using the Harajli & Mabsout (2002) bond stress – slip relationship and moment – curvature sectional analysis, applied to $24d_b$ and $36d_b$ lap splices. Deformation considered flexure and slip. Adequacy of shear strength was checked prior to the analysis to verify that shear failure did not occur prior to either reaching first yield of the column reinforcement or splice capacity.

In this study, the response of the frames using the proposed rotational spring model was found to be between the fixed and pinned base conditions with regard to roof displacement and interstory drift ratio, also termed as story drift ratio. The behavior of the frames changed depending on the yielding of the longitudinal reinforcement, as depicted by the interstory drift ratio and displacement. The performance of the building frames also depended on the ground motion. The N-S and E-W direction frame computational models considered three and four earthquakes,

respectively, totaling to 14 computational models per base condition. Three computational models out of the 14 with the proposed rotational spring base condition simulated recorded roof displacement results with accuracy. In the frame simulations where yielding of most of the column longitudinal bars was not calculated, the maximum interstory drift occurred in the upper stories, matching column damage observations during the event. The findings of the study showed that short lap splice increases the drift and displacement compared to the fixed base supporting its effect, i.e. the behavior of a non-ductile reinforced concrete case study building to an earthquake.

1. INTRODUCTION

While advances have been made towards the understanding of effects of earthquakes on structures, the risk to life safety is a prevalent issue. Seismic design codes have progressed through new knowledge and experience. Within the inventory of built infrastructure, the concern lies in existing structures designed with older codes and standards, and the seismic risk these structures pose to the society. Non-ductile reinforced concrete buildings (NDCB) are significant part of the problem, and the focus of this research. Due to the high seismic activity and available information, this thesis focuses on the state of California seismicity and relevant data.

1.1 Motivation and Background

1.1.1 Characteristics of NDCB and Design Deficiencies

Non-ductile reinforced concrete buildings (NDCB) are generally buildings built prior to mid-1970s seismic design changes to building codes. These buildings have construction details not conforming to current codes, typically using lighter amounts of transverse reinforcement and shorter longitudinal reinforcement splice lengths compared to those from current standards for seismic detailing. Throughout the 20th century, earthquake events around the world have shown the deficiencies in non-ductile reinforced concrete buildings, often resulting in irreparable damage, collapse, and most unfortunately large number of casualties. Earthquakes in California resulting in significant damage to NDCB included the 1971 San Fernando of magnitude 6.6, 1989 Loma Prieta of magnitude 6.9, and 1994 Northridge earthquake of magnitude 6.7 (Liel, 2008). In the 1971 San Fernando earthquake, the newly completed Olive View Hospital suffered serious damage to the 1st story and basement. The more significant damage consisted of the failure of multiple columns that was identified as “due to lack of confinement” (Liel, 2008).

Non-ductile detailing primarily involves lower amounts of flexural steel, transverse ties at large spacings, and inadequate tension lap lengths, corresponding to unconfined concrete and more brittle behavior. Reinforced concrete beams have detailing with bottom bars discontinuous in beam-column joints and top bars not extending sufficiently past inflection points. For reinforced concrete beams, columns, and joints, transverse reinforcement is sparsely provided, and hoops

often inadequately installed to resist seismic shear forces (Liel, 2008; Moehle, 1998). Due to earthquake events, NDCB also experienced failure in beam-column joints and columns, spalling, extensive cracking, formation of plastic hinging accompanied by longitudinal bar buckling or shear failure which may result in complete story collapses due to loss of gravity load carrying capacity. Significantly, most of the damage is owed to lack of adequate amount of transverse reinforcement (Liel, 2008).

Particularly in NDCB, in addition to the lack of closely spaced transverse reinforcement in the columns, researchers have observed the potential to experience lap splice failure due to short length of overlap of the reinforcement. Non-ductile splices are typically located right above joints typically 20 or 24 bar diameters, whereas ductile splices must be located away from critical sections such as high moment regions, ideally mid-height (Liel, 2008; Moehle, 1998). Pre-1977 code provisions for column longitudinal reinforcement, splices were designed for compression only, resulting in shorter lap lengths (J. Y. Cho & Pincheira, 2006). During earthquakes, columns develop moments putting some of the column longitudinal reinforcement in tension, which require substantially longer lap lengths than compression lap splices. Poor design of column lap-splices, normally in moment-resisting frames results in strength degradation, lack of ductility, bond deterioration, and shear failure. Due to uncertainty in the performance of the inadequate lap slices and the lack of experimental data for columns experiencing vertical collapse in NDCB, columns were assumed to fail first in shear. Liel and earlier researchers modeling building performance to earthquakes conducted the analysis assuming fixed support at the base of the building frame. This assumption does not reflect the impact on displacement demand as a result of the presence of short splices at the base of columns in NDCB. To refine and improve the performance assessment of NDCB during an earthquake, it is important to incorporate and model the performance of longitudinal reinforcement with short lap splices at the base of columns.

1.1.2 History of Code Seismic Provisions for Reinforced Concrete Building

Building code seismic provisions have been modified in the past primarily as a response to major earthquakes, with the addition of improved knowledge on the performance of existing buildings to earthquakes. In 1961, Blume, Newmark and Corning reported that reinforced concrete structures could exhibit ductile behavior through proper design and detailing. In addition to broadening the force-based design concept through ductility, Blume et. al. recommended capacity

design, avoiding sudden brittle failure by designing for a desired collapse mechanism to form hinges first in the beams. In the 1960s and 1970s, the Uniform Building Code substantially changed seismic provisions. Non-ductile reinforced concrete buildings referenced in this thesis were built before the 1970s and most likely designed using the 1967 Uniform Building Code or prior date (Liel, 2008). In the 1967 UBC, ductile detailing was not required until a minimum building height of 160 feet. By 1973 UBC, the ductile detailing characterized more closely to modern detailing and design (Liel, 2008). Included in the definition of ductile detailing, and relevant to this thesis, more stringent requirements were added regarding development length and sufficient splice length.

Earlier seismic codes provided force-based design and detailing of structures. While not directly relevant to the evolution of lap splices and development length, with more understanding of seismic design, recent decades have begun conversations about the change of concept to drift-driven design, a critical analysis parameter of this numerical simulation work as explained later. The change in design concept can provide a more in depth understanding of the evolution of seismic provisions as described by Sözen (2013).

1.1.3 Performance History of NDCB in Past Earthquakes

Non-ductile reinforced concrete buildings that have performed poorly in past earthquakes worldwide are often accompanied by significant loss of life. In California, there have been a variety of earthquakes with high magnitudes and characteristics that caused significant damage to structures. Some of the most prominent include the 1971 San Fernando and 1994 Northridge with magnitudes of 6.6 and 6.7, respectively (USGS). Other influential characteristics include soil structure interaction, proximity to earthquake epicenter, etc. Specific considered earthquake details are discussed in Chapter 3. Damage observed in NDCB structures primarily included cracking and spalling of first story columns and walls, nonstructural damage, column failure in flexure-shear and due to lack of confinement bar buckling, beam-column joint failure, pounding, and first story collapse. Figure 1.1 and Figure 1.2 display two buildings that had severe damage during the San Fernando and Northridge earthquakes, respectively. Figure 1.1 shows the first story collapse and column failure due to the lack of confinement and discontinuous walls. Figure 1.2 illustrates the failure of the second floor due to inadequate performance of the beam-column connections through lack of confinement and exterior wall not adequately tied to the building.

Figure 1.1. Olive View Hospital Medical Treatment Building
1971 San Fernando Earthquake. Damage included soft-story effect due to failure in columns and pounding to neighboring buildings. Source: (Jennings, 1971; Liel, 2008) Photo Credit: USGS Photographic Library

Figure 1.2. Kaiser Permanente Granada Hills Office Building
1994 Northridge Earthquake. Damage included second story collapse due to failure in joints and columns. Source: (Liel, 2008; Mitchell et al., 1995) Photo Credit: Mitchell et al.

1.1.4 Review of Lap Splice Detailing

The knowledge on the modeling and behavior of longitudinal column reinforcement tension lap splices used in non-ductile concrete buildings is limited. The research projects discussed in this section were mostly focused on the experimental evaluation of the behavior of NDCB columns.

Lap splices in beams tests were not considered because they do not have axial load, subjected to monotonic loads, and often tested under constant moment-beam splices, all of which do not reflect conditions for a column. Aboutaha (1994) conducted experimental tests on 28 columns with the purpose of investigating seismic retrofit of NDCB columns using rectangular steel jackets. Lynn (2001) tested three full-scale columns with detailing of lap splices found in NDCB. Melek & Wallace (2004) also conducted testing of NDCB type columns varying primary variables such as level of axial compressive load, loading history, and ratio of moment to shear. These specimens were subjected to reverse cyclic loading. The failure modes of the columns for both Aboutaha and Melek resulted in lap splice failure and yielding of reinforcing bars for Lynn (J. Y. Cho & Pincheira, 2006). NDCB typically have 20-24d_b lap splice lengths. It should be noted that ASCE41 recommended lap splice lengths greater than 35d_b for collapse prevention and 50d_b for immediate occupancy level.

A low number of analytical studies are found in the literature on the modeling of the behavior of a column with short lap splices. Bond-slip relations for single bars have been suggested and generally accepted for lapped splices (J.-Y. Cho & Pincheira, 2004; Chowdhury & Orakcal, 2012). A number of investigators have proposed bond-slip relationships of isolated bars, such as Eligehausen et al. (1983) and Harajli & Mabsout (2002). These are reviewed by Cho & Pincheira (2004) and Chowdhury & Orakcal (2012) as shown in Figure 1.3. The two types of bond failure of the lap splice, as described in the previous studies, are defined by confinement. If considered unconfined or poorly confined versus well confined, normally by transverse reinforcement, bond failure occurs with splitting of concrete versus pullout, respectively (J. Y. Cho & Pincheira, 2006). Both Cho & Pincheira (2006) and Chowdhury & Orakcal (2012) noted that use of the Harajli & Mabsout's (2002) model resulted in better and well agreement between calculated and experimental data from column test results of shear force vs. drift ratio plots. This model will also be used in this study for unconfined concrete.

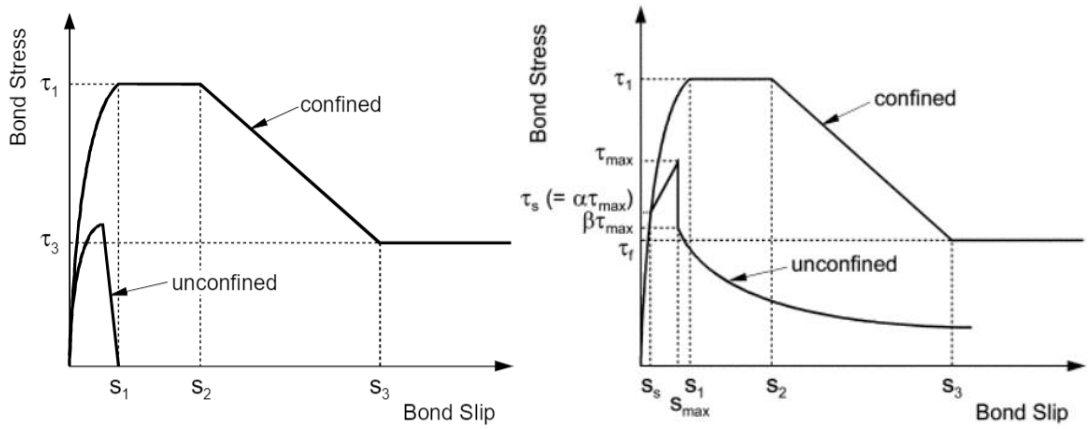

Figure 1.3. a) Local Bond Stress-Slip Relations by Eligehausen et al. (1983) and b) Harajli & Mabsout (2002)

J. Y. Cho & Pincheira (2006) and Chowdhury & Orakcal (2012) described procedures to analytically model concrete columns with short lap splices and compare analytical with existing experimental results for verification. Using a lumped plasticity model approach, termed as macroscopic modeling, Cho & Pincheira define a zero-length moment versus slip rotation spring at plastic hinge locations, indicating a rigid body motion, and considering three deformation mechanisms. Figure 1.4 displays Cho & Pincheira modeling assumption, describing the deformation mechanism of the total deflection of columns with components from modeling the connection with a flexure, shear, and bond-slip springs. Chowdhury and Orakcal use a multiple vertical line element model, formulating a fiber-based model and allowing the discretization of column element length. This approach provides finite column element lengths and differentiates two models for each discretized length, one used for the lap splice region and the other for outside the lap splice region of a column. Other investigators use similar procedures. Both J. Y. Cho & Pincheira (2006) and Chowdhury & Orakcal (2012) concluded that their analytical studies represented experimental results well. For the purpose of this thesis and applicability in SAP2000, the Cho & Pincheira model approach will be used and described in Chapter 4. In addition to the limited information on the behavior of short lap splices in the literature, there is little information on the building frame behavior and how to properly model these columns in frames.

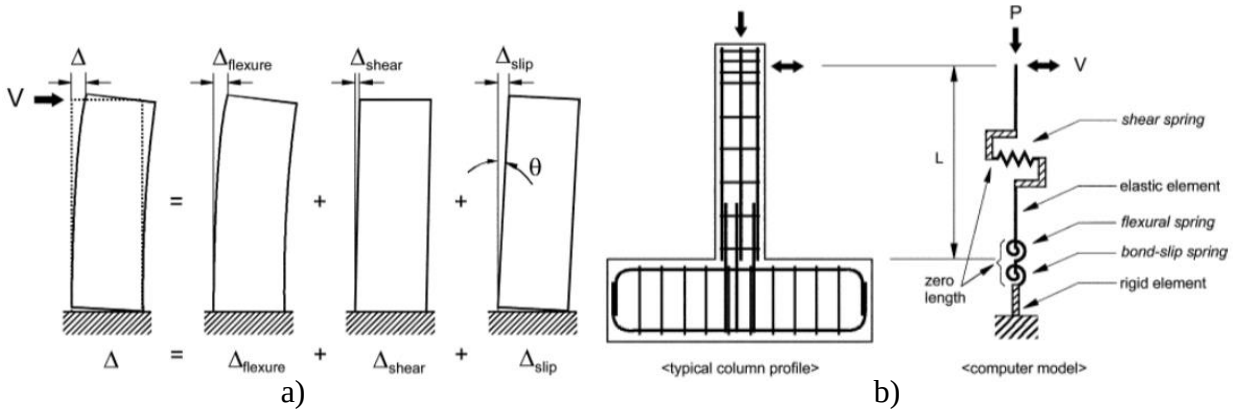

Figure 1.4. a) Deformation Mechanisms and b) Computer Model (J. Y. Cho & Pincheira, 2006)

1.1.5 Current Actions in California to Retrofit NDCB

There are approximately 1500 non-ductile reinforced concrete buildings in the city of Los Angeles alone (Baradaran Shoraka et al., 2013). NDCB and the risk they pose contribute to a prominent issue to be addressed in many communities around the world. Through what began as a study on the identification and mitigation of buildings that are considered non-ductile in UC Berkeley, Los Angeles Mayor issued "Resilience by Design" report (Office of Los Angeles Mayor Eric Garcetti, 2014) that stated a promise of action and proposed plan towards addressing the stated problem. Recently in the state of California, few cities including Los Angeles have passed or are working to pass ordinances for a retrofit mandate of NDCBs. The mandate aims to inspect all buildings that are categorized as NDCB and retrofit accordingly following a proposed timeline and requirements. The ordinances have considerable timelines on average of 25 years. These ordinances are present, but the accountability on the regulations and timelines are not enforced (LADBS, 2015). Despite the good intentions, the necessity and incentives for building owners to retrofit may not align. The concern lies in the delay or inactivity in retrofitting NDCB due to the large scope of the problem. In addition, considering all expenses are expected to come from building owners, it is unknown how proactive the owners will be.

Liel (2008) conducted research to assess the risk of NDCB in the hope of providing metrics for decision-making. Liel (2008) used performance-based earthquake engineering tools to assess the risk, where the main component included conducting non-linear dynamic analysis of archetypical buildings. While experimental data were not included in Liel's work (2008), the numerical data contributed to the understanding of NDCB.

In 2009, FEMA funded the ATC-78 project series that led to the report FEMA P-2018 titled "Seismic Evaluation of Older Concrete Buildings for Collapse Potential" (FEMA, 2018). ATC-78 project aimed to be easier and cheaper than detailed analysis procedure of ASCE 41-17. This project along with current research proposing guides for seismic evaluation are based on computational modeling. One of the main assumptions is the fixed base connection, which correlates to having adequate lap splice lengths. The main focus in this thesis is to evaluate the performance of NDCBs with inadequate tension lap slices, i.e. short lap splices, at the base of moment resisting frames.

1.2 Scope

The objective of this thesis work is to understand the impact on the performance of an NDCB of using the common assumption of a fixed foundation base connection versus the modeling of short lap splices at the base of the first story columns. A comparison between the performance of base connections, i.e. inadequate lap slices, fixed, pinned and the proposed model will be carried out and compared with the measurements of an instrumented building through several earthquakes. The building chosen for this study is the extensively studied Holiday Inn, "Van Nuys" building located in the San Fernando Valley in California. The building selected for this study was instrumented before 1971 and there is access to observed damage reports for several strong earthquakes. This study focuses to assess the impact of a short splice connection against measured values, but not to predict the performance of the case study due to the variability of external factors out of scope. Another variability factor for building behavior are the range of characteristics of a suite of ground motions. The purpose of considering a suite of ground motions is to assess the impact of different ground motions on performance of the NDCB. A general and qualitative building behavior pattern is expected and chosen to be compared quantitatively with respective roof displacement recorded data of case study for the purpose of reference. For NDCB from a retrofit standpoint, a more valuable comparison may be between roof displacements than interstory drift ratio, also termed as story drift ratio, for evaluating maximum drift and its potential for pounding to adjacent buildings. Roof displacements and interstory drift ratios are the assessment main parameters. Items not within the scope of this thesis include soil-structure foundation interaction, biaxial bending, and torsional effects.

1.2.1 Objective

The main objectives of this study are as follows:

- Propose a base connection model that best simulates the performance of a short lap splices in tension at the base connection in a NDCB through modeling of 2D frames.
- Create a computer model of the case study building using select modeling parameters in ASCE 41-17 Standard, SAP2000 software, and the proposed model of base connection, to study the building response to a set of ground motions.
- Evaluate and compare the proposed base connection model analysis results with measured response of instrumented case study building, and more importantly assess the impact of the proposed base connection to a fixed and pinned base.
- Use the numerical results to improve assessment tools for NDCB foundation connections to support efforts towards mitigating the risk to society posed by this category of buildings.

1.3 Organization

Presentation of the research effort described in this thesis is as follows:

- Chapter 2 describes the case study building, including details of the structural system, reported earthquakes and discussion on observed damage, instrumentation of the building, and brief discussion on former research efforts to analyze the Van Nuys building.
- Chapter 3 describes the assumptions and characteristics of the numerical model, including gravity load calculation, and list of earthquakes considered for the analysis.
- Chapter 4 describes the methodology, implementation, and calibration in the modeling of the tension lap splice at the base of the structure, and the discussion of results.
- Chapter 5 summarizes the objective of the study, discussion of observations and key results, along with suggestions for future work.

2. CASE STUDY BUILDING DETAILS

The case study building is referred to in the literature as the seven-story RC building in Van Nuys, and so will be referenced as Van Nuys for the thesis. It is located at 8244 Orion Avenue, in Van Nuys, California. In 1965, the building was designed by Rissman and Rissman Associates as a hotel and completed construction in 1966 (Blume, 1973). The building consists of seven floors with typical plan dimensions of roughly 62 feet by 160 feet, eight bays in the east-west direction of 18 feet 9 inches and 3 bays in the north-south direction of roughly 20 feet. Figure 2.1 shows the typical floor plan. Figure 2.2 and Figure 2.3 display elevation views of a south perimeter frame and a west perimeter frame, respectively. The 1st floor story height is 13 feet 6 inches, followed by typical height for 2nd through 6th story of 8 feet 8.5 inches, and 7th story height of 8 feet 8 inches. Total building height is 65 feet 8.5 inches. Van Nuys consists of spandrel beams throughout the perimeter and a flat slab system with varying thickness from 10 in., 8.5 in., and 8 in. at 2nd, 3rd to 7th, and roof floor, respectively (Rissman & Rismann Associated Ltd., 1965).

This case study building, as mentioned in the introductory Chapter 1, will be used to compare between the performance of the three base connections and also compare with the measurements from the recordings of the instruments with the purpose to assess the impact of a short splice connection. Apart from the characteristics from the as-built drawings of the case study, the information of the modeling characteristics and assumptions for the numerical model is stated in Chapter 3.

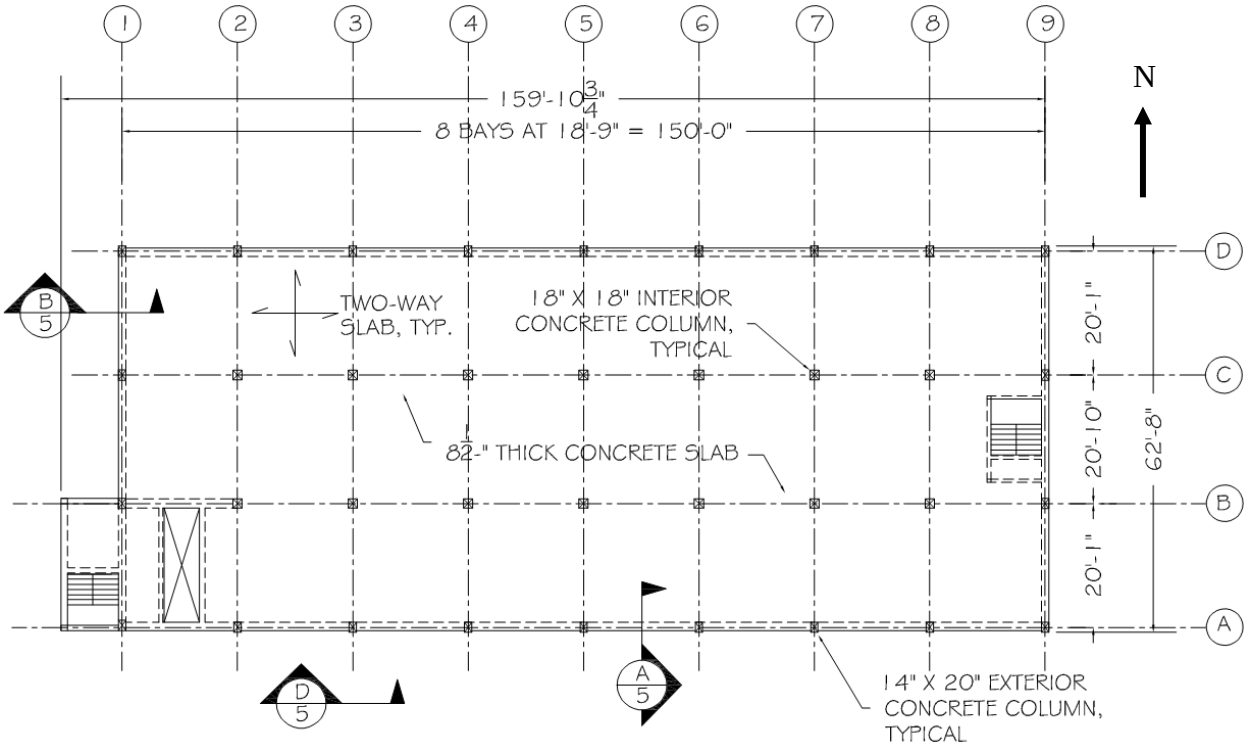

Figure 2.1. Typical Floor Plan (Rissman & Rismann Associated Ltd., 1965)

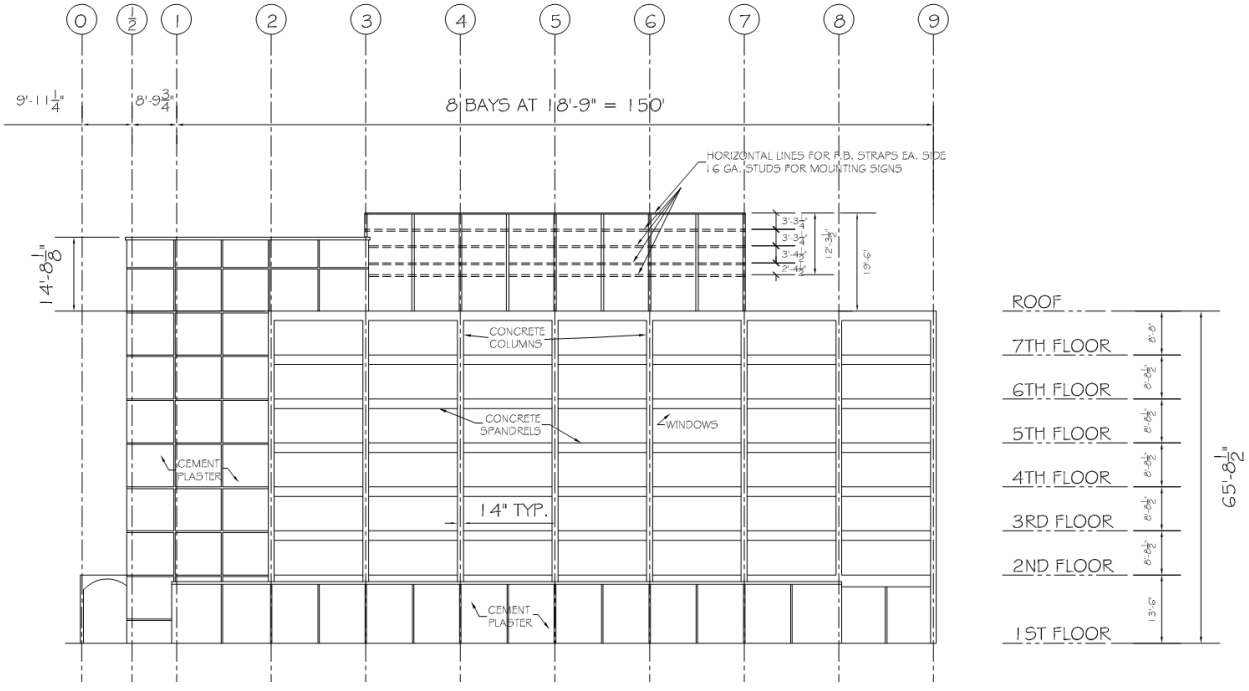

Figure 2.2. South Perimeter Frame Elevation (Rissman & Rismann Associated Ltd., 1965)

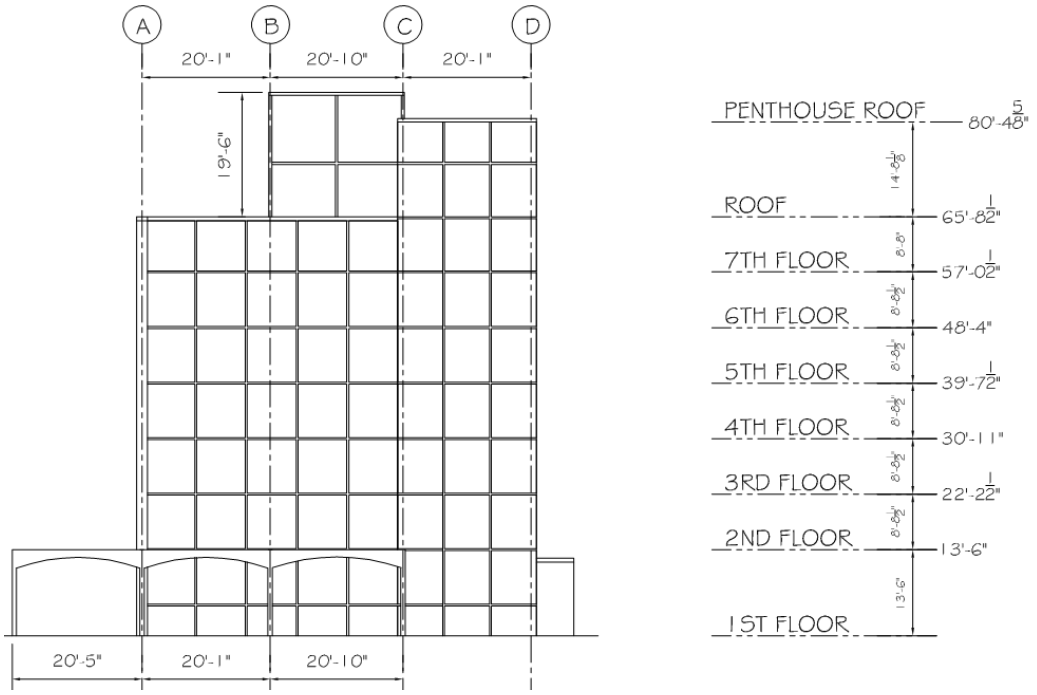

Figure 2.3. West Perimeter Frame Elevation (Rissman & Rismann Associated Ltd., 1965)

The structural system is a moment-resisting perimeter frame with non-ductile detailing. The gravity system consists of a two-way slab supported on rectangular perimeter columns and interior square columns. Typical interior column sizes are 18 in. by 18 in. and exterior columns are 14 in. by 20 in. Column schedule is shown in Table 2.1. Typical spandrel beams in the 2nd, 3rd to 7th floor, and roof are 16 in. by 30 in, 16 in. by 22.5 in., and 16 in. by 22 in., respectively. Designation for select frames in spandrel beams and interior effective beams for all floors in both orthogonal directions is shown in Figure 2.4. The beam schedule for the selected spandrel beams and effective interior beams is shown in Table 2.2 and Table 2.3. Concrete nominal compressive strength and reinforcement steel grades stated in as-built drawings are displayed in Table 2.4 and * Expected Strength due to ASCE 41-17. Refers to Section 3.2

Table 2.5. The building foundation comprises of 24 inch diameter drilled piers of two to four piers for each pile cap with lengths varying between 31.5 feet and 37 feet (Blume, 1973). Figure 2.5 displays a typical detail of column reinforcement at a beam column joint including information on typical lap splice lengths.

Table 2.1. Column Schedule

COLUMN SCHEDULE									
COLUMN MARK		C-13 to C-17, C-21 to C-26	C-11, C-12, C-20	C-4 to C-7, C-30 to C-34	C-10, C-18 C-19, C-27	C-2, C-3 C-8, C-29 C-35	C-1, C-9 C-28, C-36	C-1A, C-10A	C-17A, C-26A
LEVEL	COL SIZE	18" x 18"	18" x 18"	14" x 20"	14" x 20"	14" x 20"	14" x 20"	10" x 12"	10" x 12"
ROOF									
7th FL.	VERT. BARS	6 - #7	6 - #7	6 - #7	6 - #7	6 - #7	6 - #7	4 - #5	
	TIES	#2 @ 12"	#2 @ 12"	#2 @ 12"	#2 @ 12"	#2 @ 12"	#2 @ 12"	#2 @ 10"	
6th FL.	VERT. BARS	6 - #7	6 - #7	6 - #7	6 - #7	6 - #7	6 - #7	4 - #5	4 - #5
	TIES	#2 @ 12"	#2 @ 12"	#2 @ 12"	#2 @ 12"	#2 @ 12"	#2 @ 12"	#2 @ 10"	#2 @ 10"
5th FL.	VERT. BARS	6 - #7	6 - #8	6 - #7	6 - #7	6 - #7	6 - #7	4 - #5	4 - #5
	TIES	#2 @ 12"	#3 @ 12"	#2 @ 12"	#2 @ 12"	#2 @ 12"	#2 @ 12"	#2 @ 10"	#2 @ 10"
4th FL.	VERT. BARS	6 - #8	8 - #9	6 - #7	6 - #9	6 - #7	6 - #7	4 - #5	4 - #5
	TIES	#3 @ 12"	#3 @ 12"	#2 @ 12"	#3 @ 12"	#2 @ 12"	#2 @ 12"	#2 @ 10"	#2 @ 10"
3rd FL.	VERT. BARS	8 - #9	12 - #9	6 - #9	8 - #9	8 - #9	6 - #7	4 - #6	4 - #5
	TIES	#3 @ 12"	#3 @ 12"	#3 @ 12"	#3 @ 12"	#3 @ 12"	#2 @ 12"	#2 @ 10"	#2 @ 10"
2nd FL.	VERT. BARS	10 - #9	12 - #9	6 - #9	8 - #9	8 - #9	6 - #7	4 - #6	4 - #5
	TIES	#3 @ 12"	#3 @ 12"	#3 @ 12"	#3 @ 12"	#3 @ 12"	#2 @ 12"	#2 @ 10"	#2 @ 10"
	COL SIZE	20" x 20"	20" x 20"						
1st FL.	VERT. BARS	10 - #9	12 - #9	10 - #9	12 - #9	10 - #9	8 - #9	4 - #8	4 - #6
	TIES	#3 @ 12"	#3 @ 12"	#3 @ 12"	#3 @ 12"	#3 @ 12"	#3 @ 12"	#3 @ 10"	#2 @ 10"

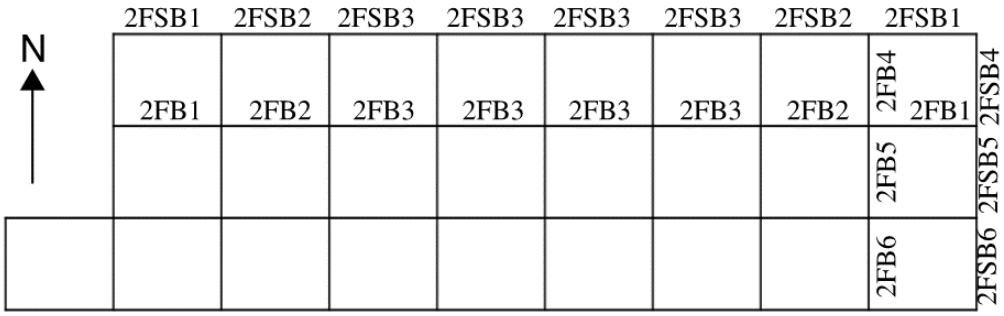

Second Floor Framing Plan

Third to Seventh Floor Framing Plan

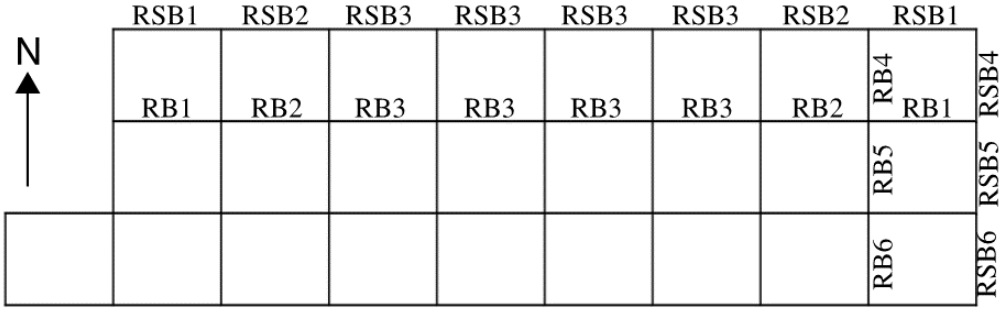

Roof Framing Plan

Figure 2.4. Framing Plans for Select Beams

Table 2.2. E-W Direction Spandrel Beams and Slab Reinforcement Schedule

E-W Direction Frame								
Spandrel Beam						Interior Beam		
Beam	*Effective Width (in)	Width (in)	Height (in)	Top Bars	Bottom bars	Beam	*Effective Width (in)	Thickness (in)
Roof								
RSB-1	3.42	16	22	2#6	2#7	RB-1	9.82	8
RSB-2	3.42	16	22	2#8	2#6	RB-2	9.82	8
RSB-3	3.42	16	22	2#8	2#6	RB-3	9.82	8
7th Floor								
FSB-1	3.42	16	22.5	2#9	2#7	FB-1	9.82	8.5
FSB-2	3.42	16	22.5	2#8	2#6	FB-2	9.82	8.5
FSB-3	3.42	16	22.5	2#8	2#6	FB-3	9.82	8.5
6th Floor								
FSB-1	3.42	16	22.5	2#9	2#7	FB-1	9.82	8.5
FSB-2	3.42	16	22.5	3#8	2#6	FB-2	9.82	8.5
FSB-3	3.42	16	22.5	2#9	2#6	FB-3	9.82	8.5
5th Floor								
FSB-1	3.42	16	22.5	2#9	2#7	FB-1	9.82	8.5
FSB-2	3.42	16	22.5	3#8	2#6	FB-2	9.82	8.5
FSB-3	3.42	16	22.5	3#8	2#6	FB-3	9.82	8.5
4th Floor								
FSB-1	3.42	16	22.5	3#8	2#8	FB-1	9.82	8.5
FSB-2	3.42	16	22.5	3#8	2#6	FB-2	9.82	8.5
FSB-3	3.42	16	22.5	3#8	2#6	FB-3	9.82	8.5
3rd Floor								
FSB-1	3.42	16	22.5	3#8	2#8	FB-1	9.82	8.5
FSB-2	3.42	16	22.5	3#9	2#6	FB-2	9.82	8.5
FSB-3	3.42	16	22.5	3#9	2#6	FB-3	9.82	8.5
2nd Floor								
2FSB-1	3.42	16	30	2#9	2#8	2FB-1	10.15	10
2FSB-2	3.42	16	30	3#8	2#6	2FB-2	10.15	10
2FSB-3	3.42	16	30	2#9	2#6	2FB-3	10.15	10

***** Effective width refers to slab, per Section 3.3

Table 2.3. N-S Direction Spandrel Beams and Slab Reinforcement Schedule

N-S Direction Frame								
Spandrel Beam						Interior Beam		
Beam	Effective Width (in)	Width (in)	Height (in)	Top Bars	Bottom bars	Beam	Effective Width (in)	Thickness (in)
Roof								
RSB-4	2.83	14	22	2#6	2#7	RB-4	9.25	8
RSB-5	2.83	14	22	2#8	2#7	RB-5	9.25	8
RSB-6	2.83	14	22	2#6	2#7	RB-6	9.25	8
7th Floor								
FSB-4	2.83	14	22.5	2#9	2#8	FB-4	9.25	8.5
FSB-5	2.83	14	22.5	3#8	2#8	FB-5	9.25	8.5
FSB-6	2.83	14	22.5	2#9	2#8	FB-6	9.25	8.5
6th Floor								
FSB-4	2.83	14	22.5	3#9	2#8	FB-4	9.25	8.5
FSB-5	2.83	14	22.5	3#9	2#8	FB-5	9.25	8.5
FSB-6	2.83	14	22.5	3#9	2#8	FB-6	9.25	8.5
5th Floor								
FSB-4	2.83	14	22.5	3#9	2#8	FB-4	9.25	8.5
FSB-5	2.83	14	22.5	3#9	2#8	FB-5	9.25	8.5
FSB-6	2.83	14	22.5	3#9	2#8	FB-6	9.25	8.5
4th Floor								
FSB-4	2.83	14	22.5	3#9	2#8	FB-4	9.25	8.5
FSB-5	2.83	14	22.5	3#9	2#8	FB-5	9.25	8.5
FSB-6	2.83	14	22.5	3#9	2#8	FB-6	9.25	8.5
3rd Floor								
FSB-4	2.83	14	22.5	3#9	2#8	FB-4	9.25	8.5
FSB-5	2.83	14	22.5	3#9	2#8	FB-5	9.25	8.5
FSB-6	2.83	14	22.5	3#9	2#8	FB-6	9.25	8.5
2nd Floor								
2FSB-4	2.83	14	30	3#9	2#9	2FB-4	9.58	10
2FSB-5	2.83	14	30	3#9	2#8	2FB-5	9.58	10
2FSB-6	2.83	14	30	2#9	2#9	2FB-6	9.58	10

***** Effective width refers to slab, per Section 3.3

Table 2.4. Compressive Strength of Concrete

f'c			
Element		**Specified Strength**	**Expected Strength***
Columns	1st Story	5ksi	7.5ksi
	2nd Story	4ksi	6ksi
	3rd Story - Roof	3ksi	4.5ksi
Beams and Slabs	2nd Story	4ksi	6ksi
	3rd Story - Roof	3ksi	4.5ksi

***** Expected Strength due to ASCE 41-17. Refers to Section 3.2

Table 2.5. Reinforcement Yield Strengths

fy		
Element	**Specified Strength**	**Expected Strength***
Columns	60ksi	75ksi
Beams and Slabs	40ksi	50ksi

***** Expected Strength due to ASCE 41-17. Refers to Section 3.2

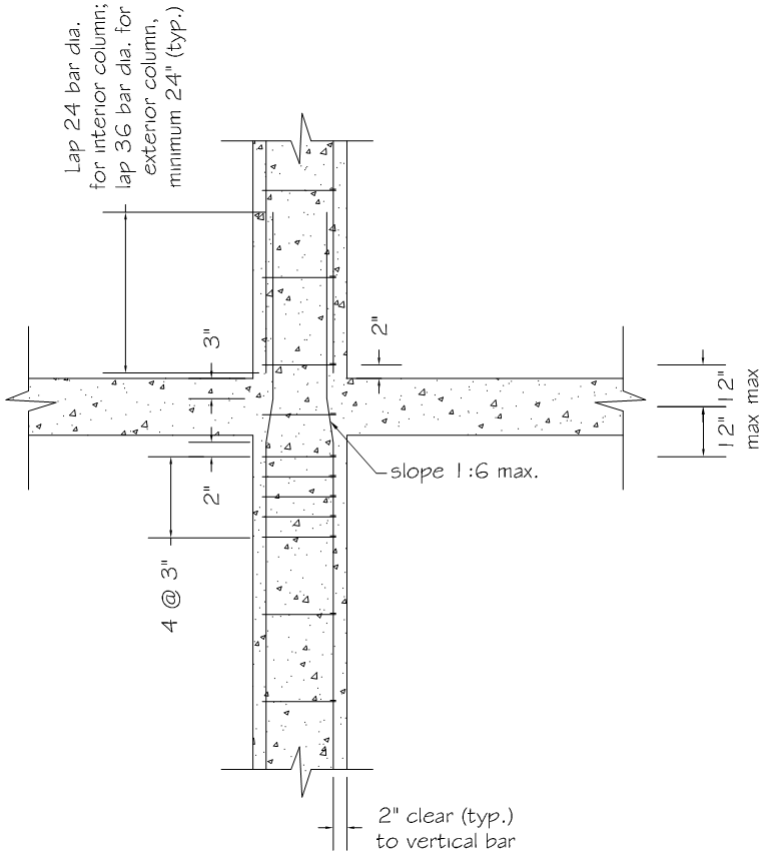

Figure 2.5. Typical Column Detail (Rissman & Rismann Associated Ltd., 1965)

2.1 Recorded Earthquakes and Observed Damage

The Van Nuys building was instrumented before the 1971 San Fernando by the California Strong Motion Instrumentation Program (CESMD). Additional accelerometers were installed in 1980s. The locations of the instruments are shown in Figure 2.6. The list of earthquakes the Van Nuys building instruments have recorded along with relevant information is shown in Table 2.6, where R is the distance from the Van Nuys case study building to each respective earthquake epicenter.

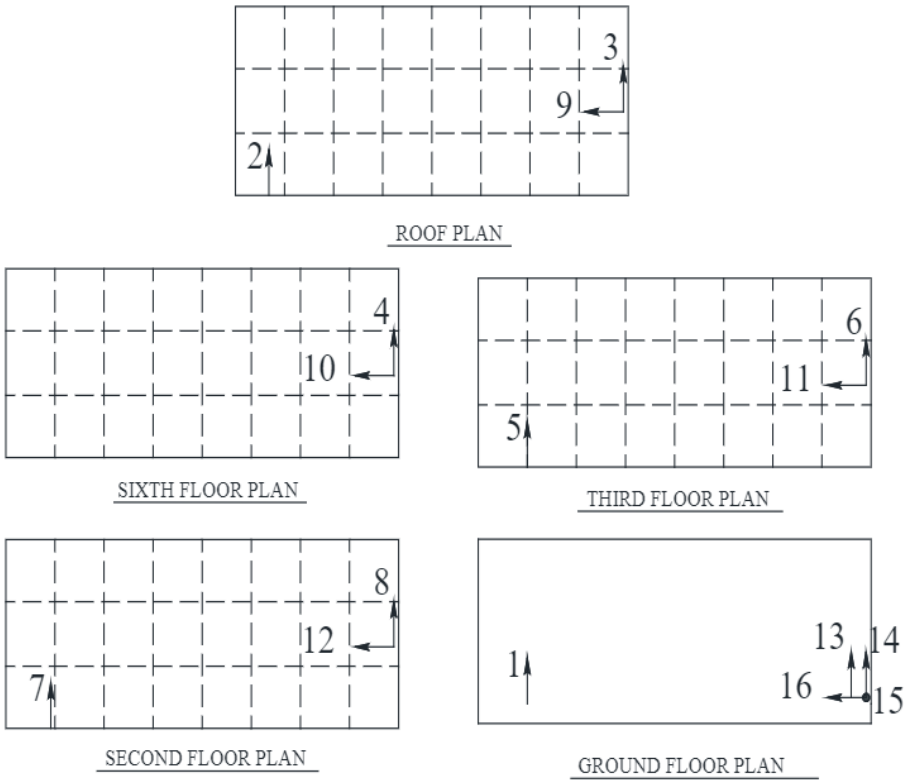

Figure 2.6. Sensor Locations after 1980s (CESMD)

Table 2.6. Earthquake Events for Case Study Building (Trifunac et. al., 1999)

Earthquake	Date	*M*	*R* (km)	*PGA* (cm/sec^2)		*PGV* (cm/sec)		*PGD* (cm)	
				Trans	Long	Trans	Long	Trans	Long
1. San Fernando	9 Feb 1971	6.6	22	240	130	27	23	5.3	9.7
2. Whittier	1 Oct 1987	5.9	41	160		8.7		1.8	
3. Whittier aft.	4 Oct 1987	5.3	38	37	52	1.4	2.2	0.3	0.3
4. Pasadena	3 Oct 1988	4.9	32	54	36	1.6	0.9	0.3	0.2
5. Malibu	19 Jan 1989	5.0	36	15	22	0.9	1.0	0.2	0.2
6. Montebello	12 Jun 1989	4.1	34	21	22	0.8	0.8	0.2	0.2
7. Sierra Madre	28 Jun 1991	5.8	44	56	62	4.6	2.8	1.0	
8. Landers	28 Jun 1992	7.5	190	41	41	12	11	6.1	4.9
9. Big Bear	28 Jun 1992	6.5	150	25	23	3.6	3.6	0.9	1.0
10. Northridge	17 Jan 1994	6.7	7.2	390	440	40	51	12	7.9
11. Northridge aft.	20 Mar 1994	5.2	1.2	270	140	7.5	4.8	0.6	0.6
12. Northridge aft.	6 Dec 1994	4.5	11	57	60	3.0	2.4	0.5	0.2

In the 1971 San Fernando earthquake, damage to the case study building was mostly architectural. Compared to all of the earthquakes listed in Table 2.6, the 1994 Northridge earthquake was the most severe in terms of structural damage to the building. The building was retrofitted after the 1994 Northridge earthquake. The structural damage concentrated in the exterior east-west direction frames. Failures included shear failure of columns and beam-column joints, spalling of concrete, buckling of longitudinal bars, and cracks observed several visible inches wide (Blume, 1973; Trifunac et. al., 1999). Trifunac et. al. (1999) reported shear failures in the columns and beam-column joints concentrated around the 3rd, 4th, and 5th stories. The observed damage patterns after the Northridge Earthquake are shown in Figure 2.7 and Figure 2.8. Relative maximum displacements and transient interstory drift ratios reported by Islam (1996) are shown in Table 2.7 for the 1994 Northridge earthquake. Other earthquakes did not cause structural damage.

In this thesis, the recorded roof displacement for selected ground motions are compared with analytical results in Chapter 4.

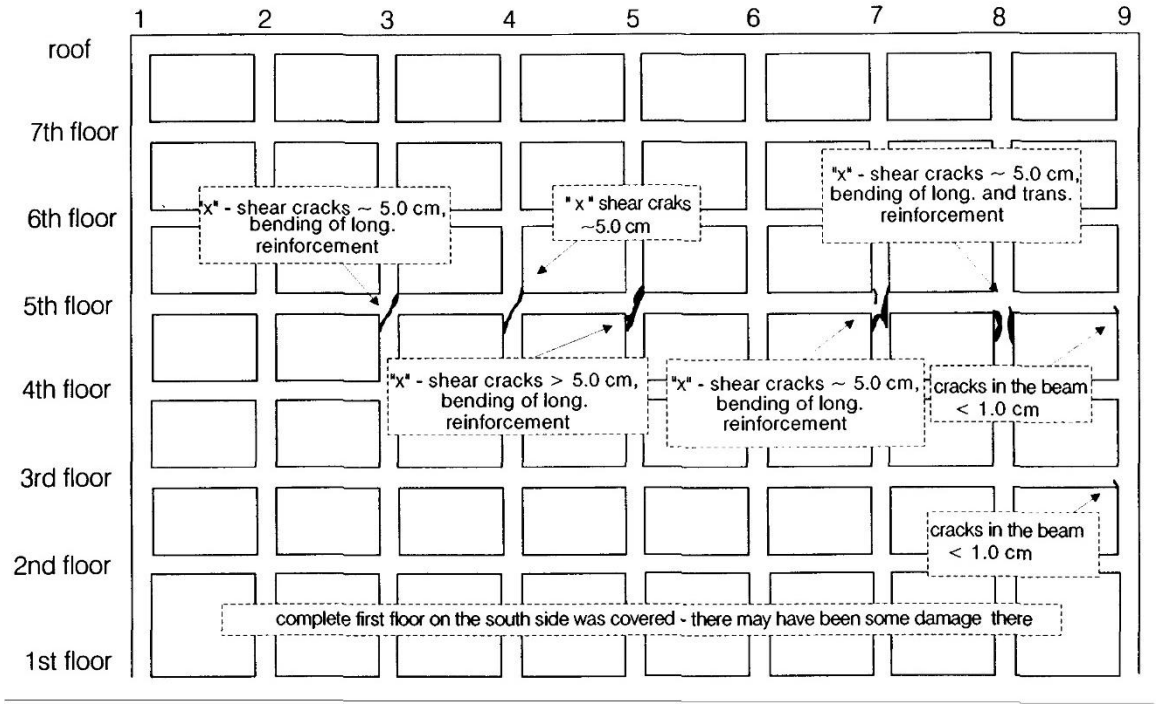

Figure 2.7. Structural Damage, South Frame (Trifunac et al., 1999)

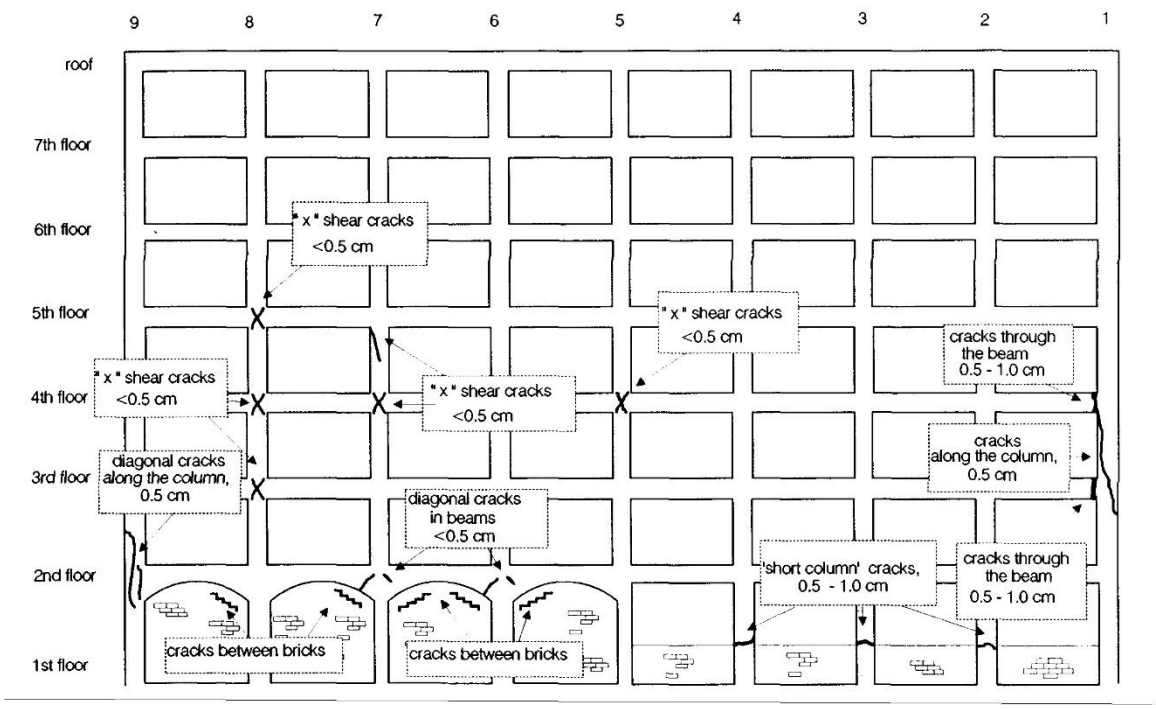

Figure 2.8. Structural Damage, North Frame (Trifunac et al., 1999)

Table 2.7. Recorded Peak Displacements and Story Drift Ratios (Islam, 1996)

Floor	Max rel. displacement (Islam, 1996)	Transient drift ratio relative to floor below Recorded (Islam, 1996)
Longitudinal		
Roof	9.2 in.	
7		
6	8.2	
5		
4		
3	3.6	1.9%
2	1.6	1.0%
Transverse		
R, east	6.9 in.	
R, west	9.0	
6, east	6.0	
3, east	2.9	1.6%
3, west	3.4	1.3%
2, east	1.6	1.1%
2, west	1.9	1.2%

2.2 Van Nuys Building Previous Studies

The case study building was previously studied by several research teams including Islam (1996), Lepage (1997), Barin and Pincheira (2002), Paspuleti (2002), and Suwal (2018). The objectives and analyses had many similarities among past studies conducted on the Van Nuys building. Using Opensees as the software framework for the numerical modeling, the shared broad objective included simulating the response of the structural system through modeling a 2D frame subjected to an incremental dynamic analysis to assess structure collapse mechanism. While the specifics regarding methodology and characteristic modeling assumptions differed between the studies, one of the consistent assumptions was to assume column bases were fixed to the ground.

Suwal (2018) studied the relationship between building damage classification in accordance to ASCE 41 and the observed damage. Results showed damage patterns were conservative with observed performance, estimating higher values than observed. Similarly, Paspuleti (2002) studied accuracy of nonlinear modeling procedures and the influence of modeling parameters. The inelastic dynamic analysis by Paspuleti failed to accurately predict most of the building response, including splice failures at the ground story columns observed in the Northridge earthquake.

Similar to the rest of the studies, while some of the building response were captured by their respective models, such as the general failure mechanism, the assumption of having a fixed base continued to be used and further suggested for future study.

3. NUMERICAL MODEL CHARACTERISTICS & ASSUMPTIONS

The objective of this research is centered around building and testing a numerical model of a non-ductile reinforced concrete structure with adequate and relevant properties. The modeling software chosen is SAP2000 for its advanced analysis capabilities. It offers a broad range of modeling options regarding material, element, consideration of nonlinearity for analysis, as well as having customizable output for post-processing results and is widely used in both professional practice and research efforts. The modeling assumptions and capabilities used are further described in this chapter. Once the numerical model was assembled, a series of ground motions were applied in the dynamic analysis of the building. In regard to the column-foundation connection, three types of connections were assumed: fixed, pinned, and "in-between" through use of rotational spring/link. Methodology further described in Chapter 4. The following modeling assumptions are listed below and are further described in this chapter:

- The building is modeled in two dimensions using typical interior and exterior frames in each principal direction.
- The beam-column joints were assumed rigid.
- The concentrated plasticity approach was used to model nonlinear behavior.
- Geometric nonlinearity, such as P-Delta effect, was considered.
- Soft story mechanism considered for hinge formation and corresponding material nonlinearity.
- Shear failures checked prior to analysis, and shear deformations consequently not included in the analysis conducted in this thesis.
- Soil-foundation interaction, biaxial bending and torsional effects not included in the analysis conducted in this thesis.

3.1 Numerical Model and Element Formulation

There are four 2D model frames built consisting of interior and exterior frames in orthogonal directions. The instrumentation of the case study building provided data for both orthogonal directions. Effective use of the data available to obtain recorded roof displacement helps understand the results of the building behavior in terms of drift as a reference to the three base

conditions of fixed, pinned, and proposed. The model of the frames is shown in Figure 2.2 and Figure 2.3 consistent with Figure 2.5 frame labels.

Two types of models for frame or element structures consist of a concentrated plasticity model and a distributed plasticity model. With the use of SAP2000, the finite element capability is used and inelastic behavior is assumed to be concentrated at the ends of structural members, assuming a concentrated plasticity approach.

All four frames have column and beam elements, where beams consist of slab only or slab-beam to account for stiffness and mass of the structure. Column and beam elements are defined with properties from Table 2.4 and * Expected Strength due to ASCE 41-17. Refers to Section 3.2

Table 2.5, allowing input of reinforcement details of columns and beams. Loading was applied to the model, in accordance to Table 3.3.

3.2 Material Properties

The software SAP2000 has three options for concrete stress-strain models: simple, Mander, and user-defined. The simple stress-strain model, as shown in Figure 3.1a, parabolic portion follows Hognestad parabolic equation and the linear portion follows a linear relationship till 0.2f`c stress reduction and a respective ε_u of 0.005 (Computers and Structures Inc., 2008). The tensile yield stress is $7.5\sqrt{f'c}$. In regards for the reinforcement steel stress-strain model, the options include simple, Park, and user-defined. The simple stress-strain model includes elastic, perfectly plastic, and strain hardening regions as shown in Figure 3.1b. For the research objective needs, simple stress-strain models for both concrete and reinforcement were chosen.

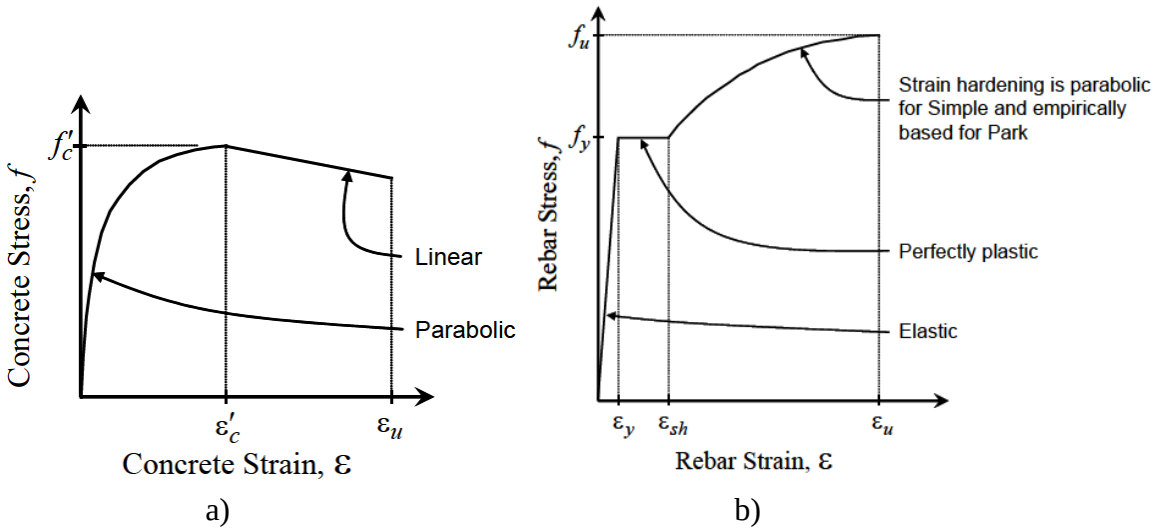

Figure 3.1. a) Concrete Stress-Strain Curve and b) Reinforcement Steel Stress-Strain Curve (Computers and Structures Inc., 2008)

The case study building, Van Nuys, uses normal weight concrete. To account for typical observed material over-strength, factors in Table 3.1 from ASCE41-17 provisions were used to calculate expected strengths. Over-strength of concrete is due to age or required over-strength at casting (Paspuleti, 2002). The specified strengths and expected strengths are shown in Chapter 2 in Table 2.4 and * Expected Strength due to ASCE 41-17. Refers to Section 3.2

Table 2.5. Past Van Nuys project researchers Paspuleti (2002) and Suwal (2018) used factors to account for material overstrength.

Table 3.1. ASCE 41-17 Material Strength Factors

Material Property	Factor
Concrete compressive strength	1.5
Reinforcing steel tensile yield strength	1.25

3.3 Effective Beam Width and Spandrel Beams

The four interior or exterior frames in consideration are two-dimensional frames with defined widths. The two-dimensional frames have the “beam” element with an equivalent width, defined as distance midspan to midspan of adjacent spans, and an effective beam width, defined

as the slab width used to consider in stiffness calculations. Due to previous research supporting that frames subjected to dynamic and cyclic loading experience larger rotations in the slab strip near the columns rather than slab centerlines, the entire equivalent width does not contribute to the stiffness. For the interior frame, the slab only contributes to the stiffness, whereas for the exterior frame the slab and beam are considered. The slab-beam element has the same thickness as the original slab thickness. ASCE41-17 recommends using the equations shown below for defining the effective beam width, based on Hwang and Moehle (2000). In addition to account for cracking from temperature, nonlinear response, or shrinkage, an effective stiffness factor β_{eff} should be used for gross section properties to reduce slab stiffness. There is general agreement to take β_{eff} as 1/3 (ASCE 41, 2017), used as well by Suwal (2018). SAP2000 uses this "beam" element defined with this effective width, and the addition of the actual beam on the column centerline for the exterior frame or namely the spandrel beam, for stiffness calculation. The rest of the slab equivalent width not considered in the effective beam width is treated as additional gravity loading, discussed later in section 3.7.

$b_{eff} = 2c_1 + l_1/3$	for interior frames	Equation 3.1
$b_{eff} = c_1 + l_1/6$	for exterior frames	Equation 3.2

Where,

b_{eff} = effective beam width

c_1 = column size parallel to the span

l_1 = center to center span length in the direction

3.4 Beam-Column Joints

The objective of the study is based on the assumption that the foundation connection, region with inadequate lap splice length, is not rigid and rather allows rotation. With rotation at the base allowed, a decrease in the forces of the beam-column joints is assumed. While the beam-column joints experience shear deformations, they are low and negligible when compared to those at the base. Therefore, the frame models assume joints to be rigid.

3.5 Stiffness of Beams and Columns

According to ASCE 41-17, effective stiffness values are considered for calculating the initial period of the building and providing better accuracy for the internal distribution of forces. The reduction factor for columns depends on the axial load demands. The effective stiffness accounts for the softening effect due to cracking in the sections experiencing dynamic motion. Table 3.2 displays the reduction factor values considered in this study taken from ASCE41-17. ASCE41 is the standard for evaluation and rehabilitation procedure of existing reinforced concrete buildings. Nonlinear parameters are defined in ASCE41 developed through NIST reports and other supporting research that helped identify potential collapse indicators, which formed the analysis procedure and nonlinear parameter values (Holmes, 2014).

Table 3.2. ASCE 41-17 Effective Stiffness

Component	Flexural Rigidity
Columns with compression due to design gravity loads $\geq 0.5A_g f'c$	$0.7E_cI_g$
Columns with compression due to design gravity loads $\leq 0.5A_g f'c$ or with tension	$0.3E_cI_g$
Beams-nonprestressed	$0.3E_cI_g$

3.6 Modeling of Nonlinearity, Hinge Formation and SAP2000 Time History Procedure

Material nonlinearity is considered for the frames where the proposed rotational springs are applied at the foundation base. Chapter 4 discusses the proposed rotational springs modeling the inadequate lap splice lengths. Frames with fixed or pinned base conditions do not have hinges defined. The frames with rotational springs act as a limited rotation hinge defined at the base due to the assumption of soft story mechanism. Among NDCB, the greatest concern and observation is a brittle failure in the columns, also known as soft story mechanism or weak column, strong beam. With the considered mechanism, hinges form in the columns first. The hinge consisting of a rotational spring applied at the base connection will govern the behavior and decrease flexure and shear forces on upper stories, resulting with only considering the base hinge in the model. Geometric nonlinearity is considered in SAP2000 by using direct integration solution when running the nonlinear time-history analysis through P-Delta effects. The other solution type of

modal analysis only allows consideration of material nonlinearity, although allows for a simpler and faster solution. To consider the state before a ground motion, where the case study experienced gravity loads, the initial conditions were continued from a state at the end of a static load case, i.e. the gravity loads. Hence, the analysis type in SAP2000 considered is nonlinear. Through running the modal load case, considering gravity loads on the structure and contributing to the mass and stiffness, the initial period of the building was obtained for each ground motion. A damping of 5% was used for all models. Other researchers studying the Van Nuys structure considered in this thesis have used similar estimate for damping, and assumed to be typical for NDCB. Using direct integration method of dynamic analysis specifies the use of mass and stiffness proportional damping, known as Rayleigh damping, instead of modal damping as used in an elastic analysis. The mass and stiffness proportional damping in SAP2000 allows to define the damping of 5% for the rotational spring base models. SAP2000 calculates the damping factors through the inputs of the initial two periods, i.e., from the first and second mode of vibration of the modal load case. Upon these modifications to the load cases, then the time history analysis for each ground motion were conducted and thereafter analyzed, as discussed in following chapters.

3.7 Gravity Loads

Gravity loads were estimated based on as-built drawings and typical loadings. Suwal (2018) derived the estimates as shown in Table 3.3, including some extra typical estimates for columns and beams, and applied the loading at each floor. Gravity loads also included 25% of unreduced live load specified in ASCE7-10. The models in this study had the loading shown in Table 3.3 applied, multiplied by respective widths for linear distribution load. Table 3.3 does not show self-weight values. The defined member elements in the frame models allowed SAP2000 to calculate the self-weight loads. A 150pcf unit weight of concrete was used in all self-weight calculations. Other additional loads were calculated using a spreadsheet to produce linear distributed loads. Adequate moments from the loads due to the remaining width and not the effective beam width were also calculated and applied.

Table 3.3. Additional Gravity Loads

Additional Gravity Loads	Roof	7th	6th	5th	4th	3rd	2nd
	psf	psf	psf	psf	psf	psf	psf
Live Load	--	10	10	10	10	10	10
Roofing	15	--	--	--	--	--	--
Electrical and Mechanical Equipment	5	5	5	5	5	5	5
Partitions	5	10	10	10	10	10	10
Flooring & Ceiling	10	15	15	15	15	15	15
Total Additional Gravity Load	35	40	40	40	40	40	40

3.8 Shear Strength Check of Columns

Shear is a brittle mode of failure for RC columns, especially those considered nonductile. It is especially catastrophic when the shear failure is accompanied by a loss of gravity load capacity. Through a comparison of shear demand to shear capacity of a column and the use of ASCE41-13 classification, shear is checked. The shear demand is calculated to represent the maximum probable shear force, calculated as the worst case when ends are fixed. The east-west direction frames values are shown in Figure 3.2 and Figure 3.3, calculated assuming fixed base for observation of considered critical case. Calculation details are provided elsewhere (Suwal, 2015). Due to same material properties and shear calculation procedures, values are equal to Suwal (2015). Table 3.4 displays the classification by ASCE41-13, removed in ASCE41-17, classifying condition i, ii, and iii as flexure, flexure-shear, and shear failure, respectively. These categories are expressed to be conservative. It is observed most columns are expected to fail first in flexure, with the few exceptions as demonstrated by the observed shear cracks in beam-column joints in the 3rd, 4th, and 5th floors in the exterior frame for the 1994 Northridge earthquake and Figure 3.3 for the interior frame.

Table 3.4. ASCE 41-13 Column Failure Classification

Shear Capacity Ratio	ACI 318 Conforming Seismic Details with 135-Degree Hooks	Closed Hoops with 90-Degree Hooks	Other (Including Lap-Spliced Transverse Reinforcement)
$V_p/V_o \leq 0.6$	i[a]	ii	ii
$1.0 \geq V_p/V_o > 0.6$	ii	ii	iii
$V_p/V_o > 1.0$	iii	iii	iii

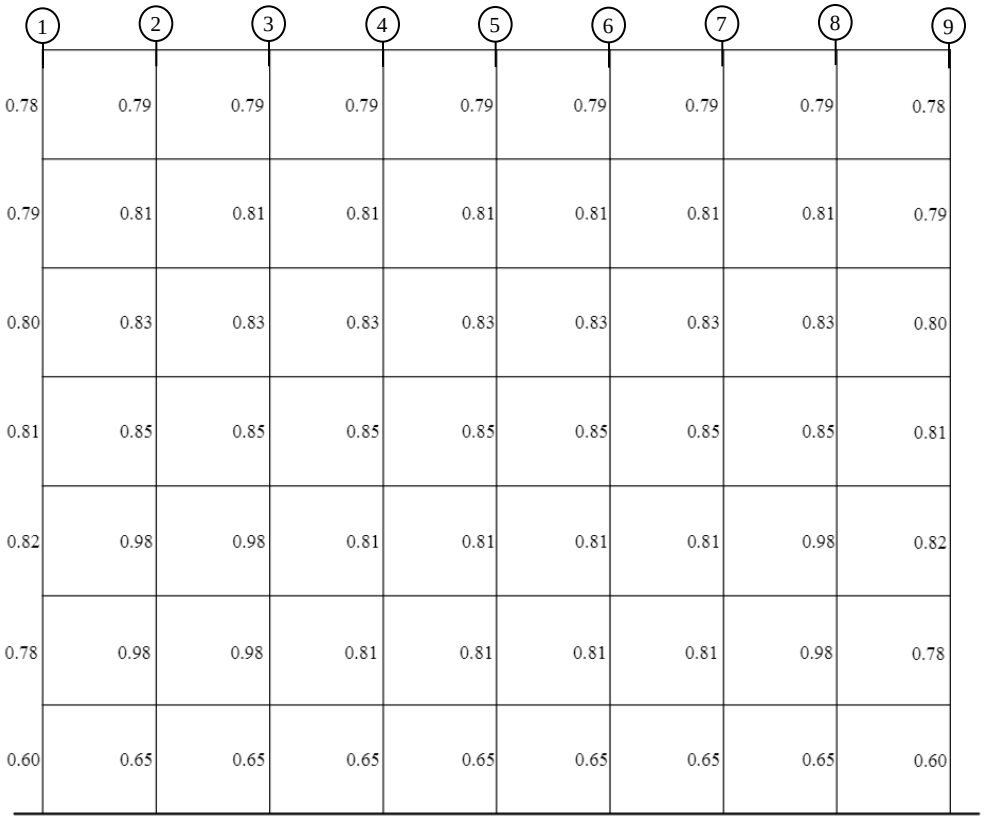

Figure 3.2. V_p/V_o Ratio for Exterior Frame (Suwal, 2015)

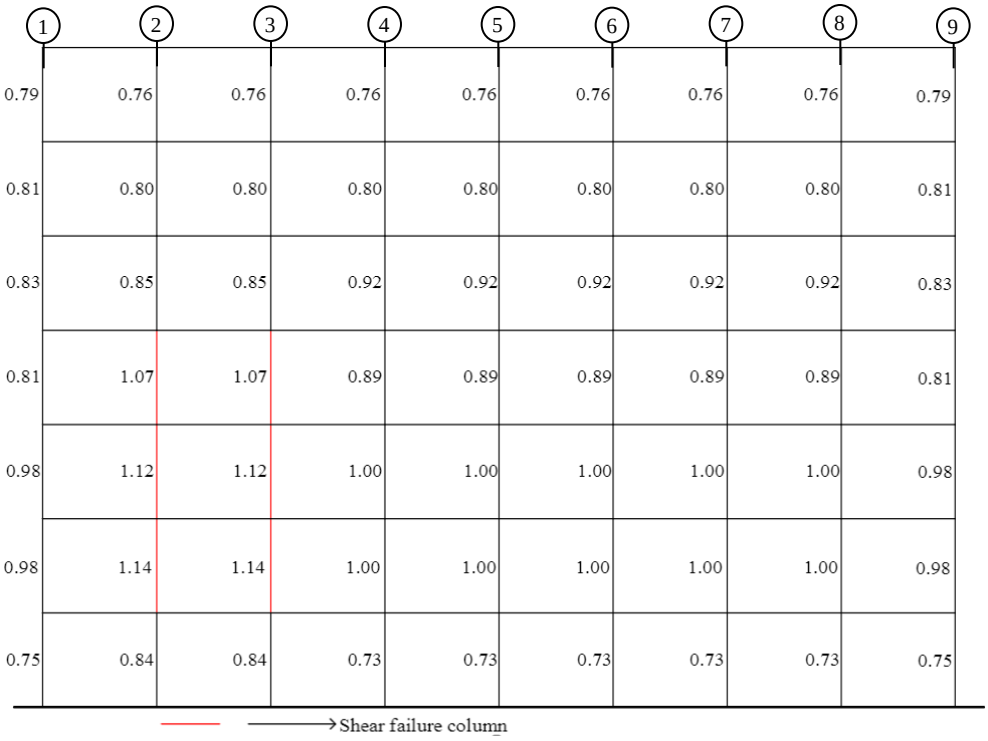

Figure 3.3. V_p/V_o Ratio for Interior Frame (Suwal, 2015)

3.9 Earthquakes Considered

There are several ground motions recorded for the Van Nuys case study building. Four ground motions were chosen to conduct the numerical model analysis described in Chapter 4. These four had the largest magnitudes in the list, but varied in response, as shown through the spectra plots. The four ground motions are listed in Table 3.5. San Fernando and Northridge earthquakes resulted in nonstructural and structural damage. Whittier and Landers had considerably lower intensities and did not cause significant damage. A total of seven ground motions were used, three in the E-W direction and four in the N-S direction. Through the building instrumentation, records for ground and roof levels were obtained and used in the analysis and implementation, further shown in Chapter 4. Figure 3.4 and Figure 3.5 display acceleration and displacement spectra that correspond to a damping ratio of 5%. Ground motion records for the Van Nuys building are available from Center for Engineering Strong Motion Data (http://www.strongmotioncenter.org).

Table 3.5. Ground Motions Information

Events	Year	Magnitude (M)	R (km)	PGA	
				E-W	N-S
San Fernando	1971	6.6	22	0.13g	0.26g
Landers	1992	7.5	186	0.04g	0.04g
Whittier	1987	5.9	41	Not Recorded	0.16g
Northridge	1994	6.5	1.5	0.45g	0.39g

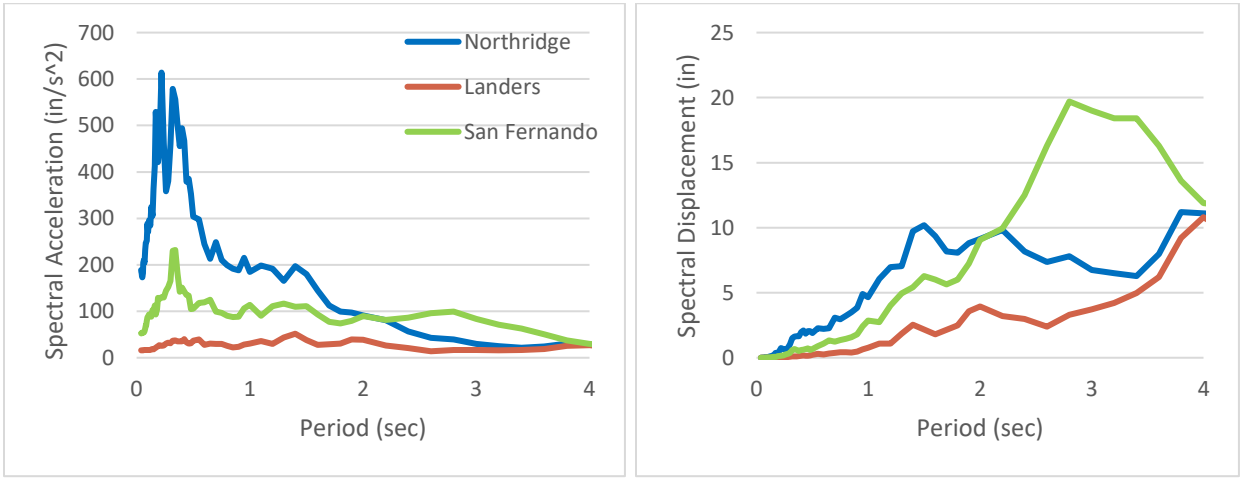

a) b)

Figure 3.4. a) E-W Frame Acceleration Spectra and b) Displacement Spectra

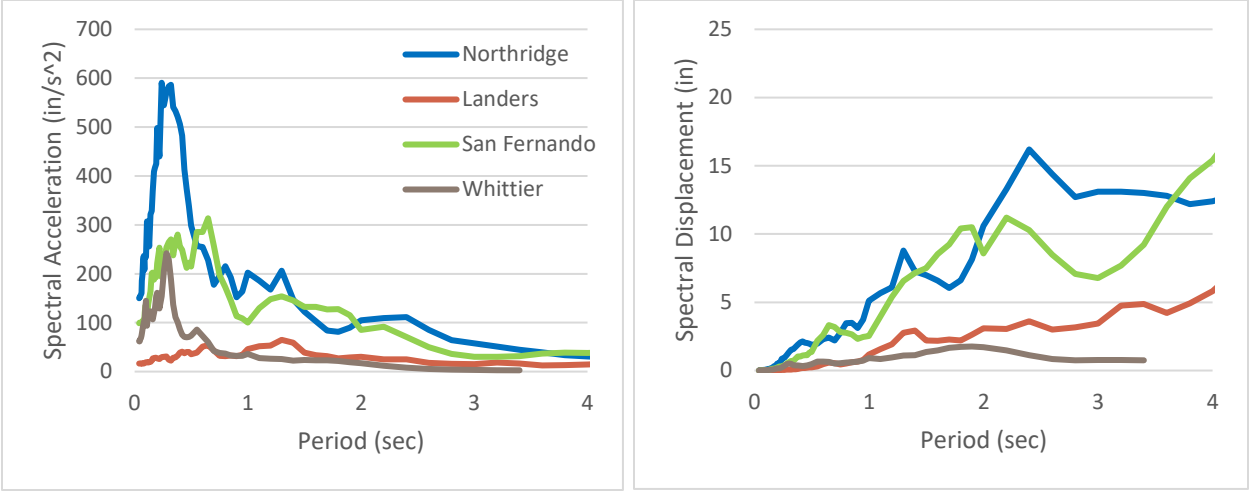

a) b)

Figure 3.5. a) N-S Frame Acceleration Spectra and b) Displacement Spectra

4. DYNAMIC ANALYSIS, IMPLEMENTION & RESULTS

Existing practices for modeling buildings or individual columns with short lap splices are limited. As previously mentioned in Chapter 2, modeling NDCB commonly included a fixed base assumption. This assumption is based on existing and up to date design practices for the building to behave in a desirable manner, also known as strong column, weak beam. Considering NDCB do not meet current building standards, the base connection is not expected to behave fixed, but rather allow rotation. Through allowing rotation at the base, concern is expressed in the consequent change of the building behavior to a soft story mechanism due to a more sudden yielding of the longitudinal reinforcement. The mechanism forms by forming plastic hinges in the top and bottoms of the columns in the first story, assuming no shear failure occurred, resulting in the majority of drift taken by the first story columns that can result in sudden failure associated with loss of gravity load carrying capacity or stability due to excessive deformation of the columns. To study the effect of different boundary conditions on drift estimation of the Van Nuys case study building, fixed, pinned, and a proposed rotational spring foundation boundary conditions are explored for a suite of ground motions.

4.1 Dynamic Analysis Methodology

The limits of the boundary conditions of the building base are fixed to pinned. The case study building model is run with both all fixed and all pinned base conditions for three ground motions in the E-W frames and four in the N-S frames. As shown in Figure 1.4, a rotational spring is implemented in the modelling of the short lap splice to account for the slip due to the rotational spring. The total drift of the column is defined as the sum of deformation due to flexure and slip. A separate strength check is conducted to determine if the column is expected to fail in shear. SAP2000 accounts for calculating flexure deformations with the definition of the element members and the slip is defined through a rotational spring. The shear deformations are considered negligible when compared to the other deformations if the columns are not shear deficient with respect to strength. The implementation of the rotational spring for deformations due to short lap splice, i.e., slip was checked through comparison of calculated and measured response of one column tested by Cho & Pincheira (2004) model. In this reference 14 columns were tested to

develop the model. The details of the columns tested were representative of columns found in NDCB. After moment versus rotation results were confirmed, frame columns were calibrated to the model. To model the rotational spring, a nonlinear multilinear plastic type link was defined in SAP2000, with the selection of Takeda hysteresis type and defined moment – rotation relationships obtained from the calibration for each base column in the frames.

There are two main perspectives for looking at the results: (i) comparison of the three base conditions, and (ii) the performance of the case study building for a suite of ground motions.

For the performance, the frames results are compared against recorded roof displacements corresponding to respective ground motions, in addition to the fixed and pinned results. The Van Nuys building was instrumented before the San Fernando earthquake. Description of instrument locations on the building are shown in Figure 2.6. Acceleration time histories were recorded by accelerometers and displacement time histories were obtained through numerical integration (Shakal & Huang, 1985). More details in Section 3.9. The recorded roof displacement time histories are available for each ground motion and are subsequently used for comparison of results.

4.2 Implementation of Proposed Rotational Spring Model

The rotational spring characteristics are derived through two relationships: bond stress – slip of the lap spliced bars and moment – curvature of the column member. The bond stress vs slip relationship used is the Harajli & Mabsout's (2002) Model, as described in Section 1.1.4. The moment – curvature relationships was obtained through sectional analysis in SAP2000. Bond-slip relations have inputs of concrete compressive strength, longitudinal bar diameter, lap splice lengths, and concrete cover. The characteristics of the columns described in Van Nuys and generally in NDCB are poorly confined, hence the bond failure that corresponds is splitting failure. Figure 4.1 displays the local bond stress vs local slip model, along with a few defining curve equations and parameters. Harajli & Mabsout looked at both plain concrete and fiber reinforced concrete. Using the equations provided and input parameters, the curve as shown for splitting failure for plain concrete was generated for each column member at the base of the frame. The model was based on an iterative procedure and discretization of the bar splice length, using the stress-strain and local bond stress-slip relationships of the reinforcing bars to calculate the stress, force, and slip at the end of the bar lap splice. The stress-strain for the reinforcing bars are assumed

to be linear elastic perfectly plastic due to strain not reaching strain hardening for the case of short lap splices such as those in these columns.

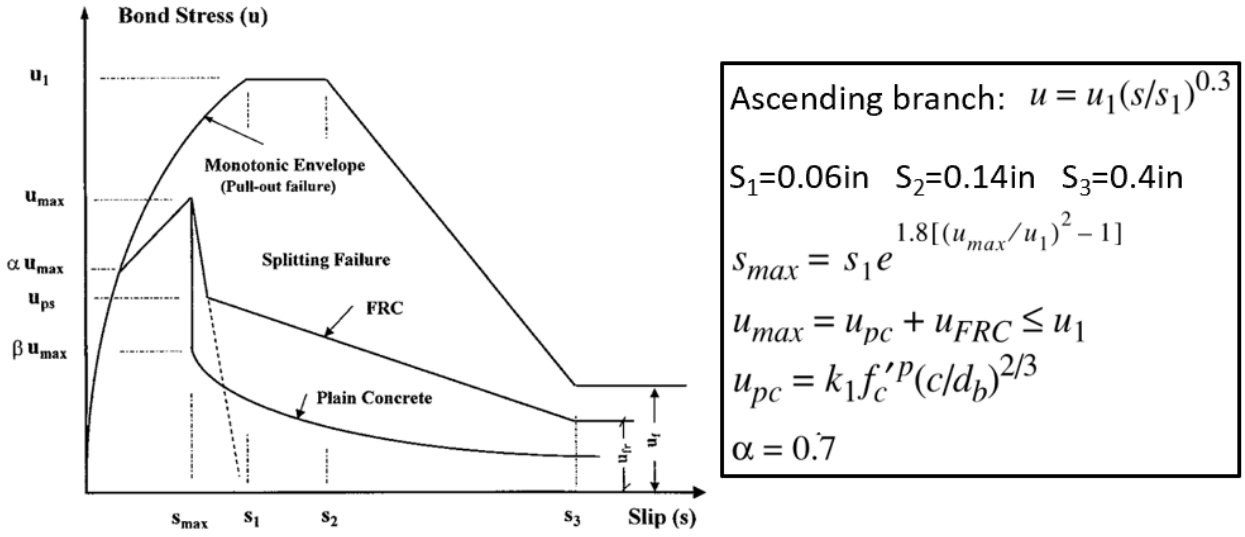

Figure 4.1. Harajli & Mabsout (2002) Local Bond Stress vs. Slip Model

Harajli & Mabsout local bond stress – slip curve is derived empirically. The variables k_1 and p are derived constants. Variable c and d_b are concrete cover and longitudinal bar diameter, respectively. Appendix A provides a few more details and one column results for one frame column. Both moment – curvature and bond stress – slip relationships are required to develop the moment – rotation relationship of a column element. Figure 4.2 displays how to relate slip to rotation, as described by Barin & Pincheira (2002). As previously described, several researchers including Cho & Pincheira (2004) studied the method described and compared against experimental results of 14 column data with short lap splices. Calculations were repeated for one column to check the observed modeling procedure and plot results were actually represented as calculated, results shown in Figure 4.3. In the reference, additional validation of the parameters in this model was conducted in the work of Cho & Pincheira (2004).

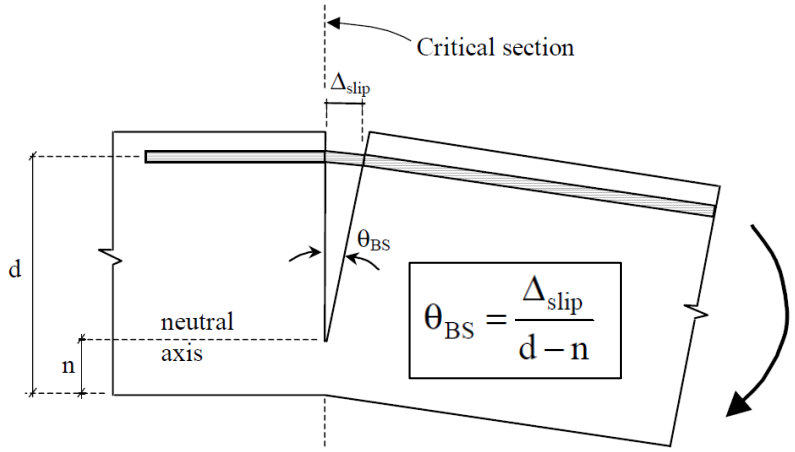

Figure 4.2. Barin & Pincheira (2002) Rotation Calculation

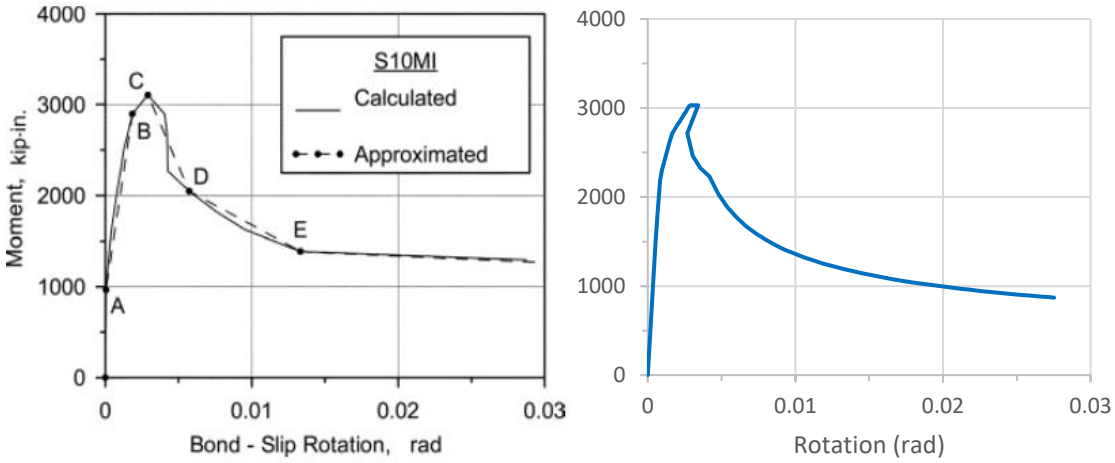

Figure 4.3. a) S10MI Column Moment – Rotation Results from Cho & Pincheira (2004), and b) Calculated Results

4.3 Case Study Building Period

Through a modal analysis, the building fundamental period for the two frames was calculated with each of the three boundary conditions considered. As seen in Table 4.1, the fundamental period of the Van Nuys building varies depending on the direction and boundary condition, where we observe the proposed rotational spring provides a value between fixed and pinned. The fixed base condition period is consistent with the values obtained by other researchers (Suwal, 2018).

Table 4.1. Building Period (secs)

	E-W Int.	E-W Ext.	N-S Int.	N-S Ext.
Fixed	1.76	1.15	1.83	0.98
Pinned	2.31	1.67	2.42	1.30
Proposed	1.80	1.22	1.87	1.03

4.4 1994 Northridge Earthquake Ground Motion

The Northridge earthquake has a duration of 60 seconds. Figure 4.4 and Figure 4.9 shows the roof displacement time history for the recorded values and the three base conditions in the two frame directions. The results show the fixed and pinned conditions overestimating or underestimating the displacement values, whereas the proposed rotational spring results are in a better agreement with the recorded values for the E-W and N-S interior frame. The exterior frame analysis results in a similar observation for roughly the first ten seconds for the E-W direction, and low agreement for the N-S frame. Figure 4.5-Figure 4.6 and Figure 4.10-Figure 4.11 display the relationship of the Interstory Drift Ratio (IDR) at max roof displacement with respective values for subsequent stories and the maximum interstory drift ratio for each story. The results show the difference in behavior between pinned, fixed, and proposed rotational spring models. The proposed rotational spring interstory drift ratio values, for the most part, lie between fixed and pinned base condition as expected. Specifically, in the E-W direction for the first story, the IDR for pinned is about three times that of fixed. Whereas the estimated values in the first story using the fixed assumption are around 25% less than those obtained using the proposed rotational spring for the interior frame, and 30 to 40% less in the exterior frames. In the N-S direction, the estimated values in the first story using the fixed assumption are 30% less than those obtained using the proposed rotational spring for the interior frame, and around 45% less in the exterior frame, both of which are greater differences than in the E-W frame. Figure 4.7-Figure 4.8 and Figure 4.12-Figure 4.13 provide two plots that display the maximum displacement values for each story and relationship between roof displacement and base shear comparing the proposed three base conditions. The maximum displacement always occurs at the roof, but the behavior of the intermediate floors change shape according to the response. The base shear decreases as base condition goes from

fixed to proposed and then to pinned. The base shear was calculated by the summation of the horizontal forces at the base of the frame and followed for all ground motions.

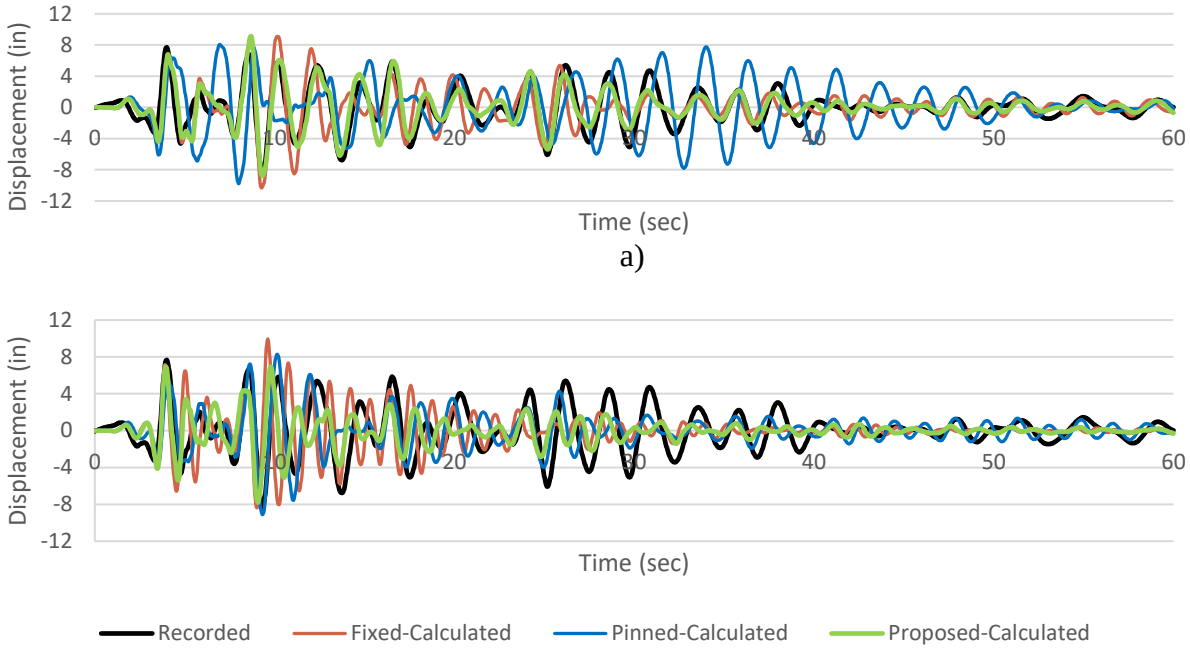

Figure 4.4. a) Roof Displacement Time History for E-W Interior Frame – Northridge and b) E-W Exterior Frame – Northridge

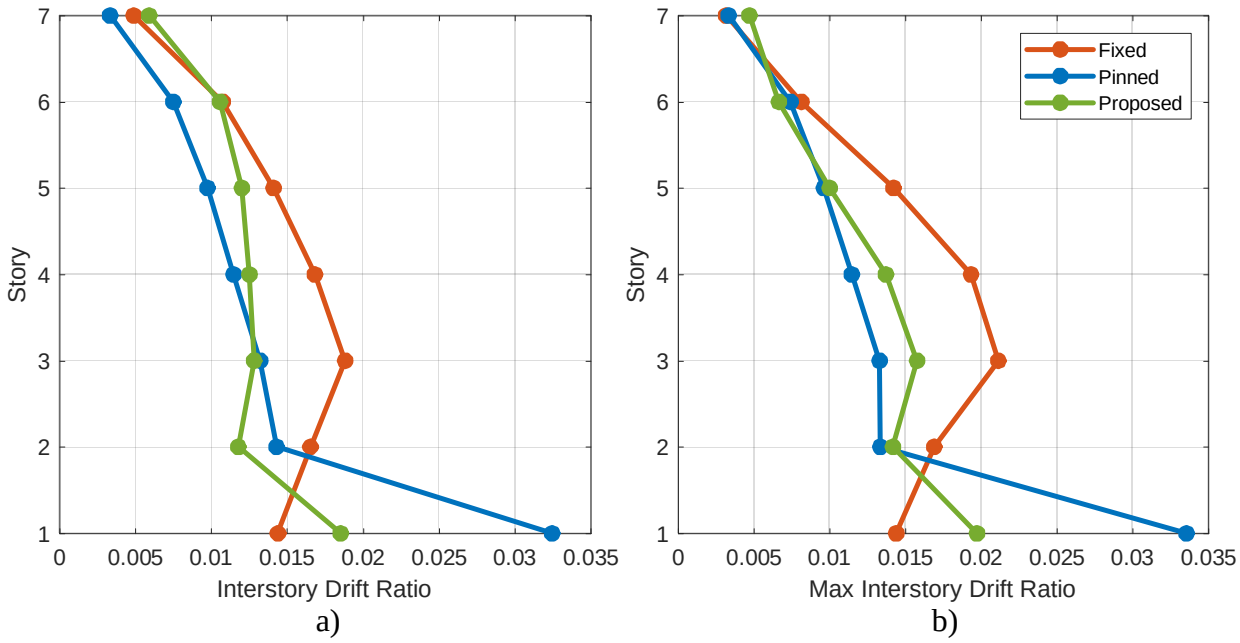

Figure 4.5. a) E-W Interior Frame IDR: Interstory Drift Ratio (IDR) at max roof displacement, and b) Max IDR: the maximum interstory drift ratio for each story – Northridge

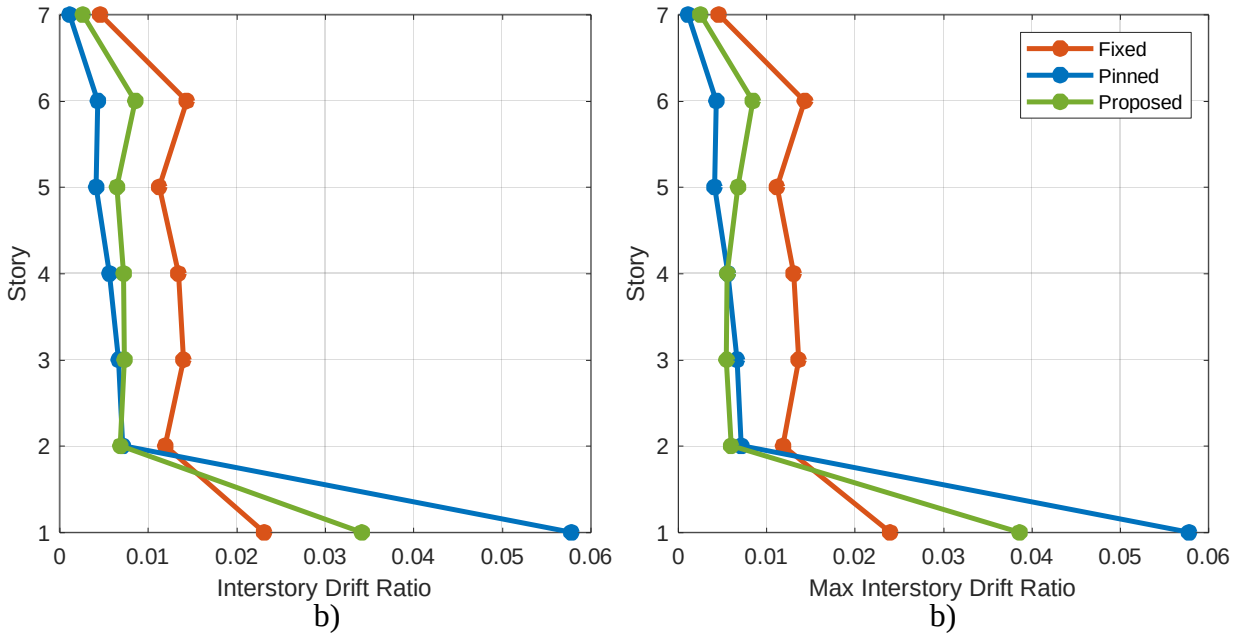

Figure 4.6. a) E-W Exterior Frame IDR: Interstory Drift Ratio (IDR) at max roof displacement, and b) Max IDR: the maximum interstory drift ratio for each story – Northridge

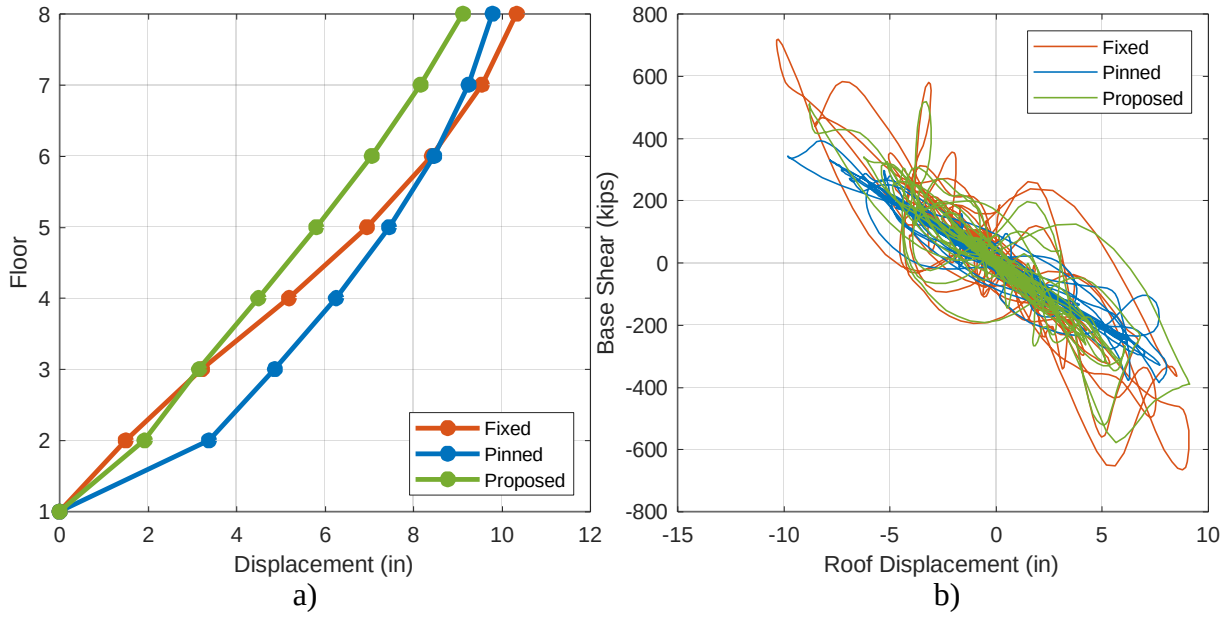

Figure 4.7. a) E-W Interior Frame Maximum Displacements per floor and b) Base Shear vs. Roof Displacement – Northridge

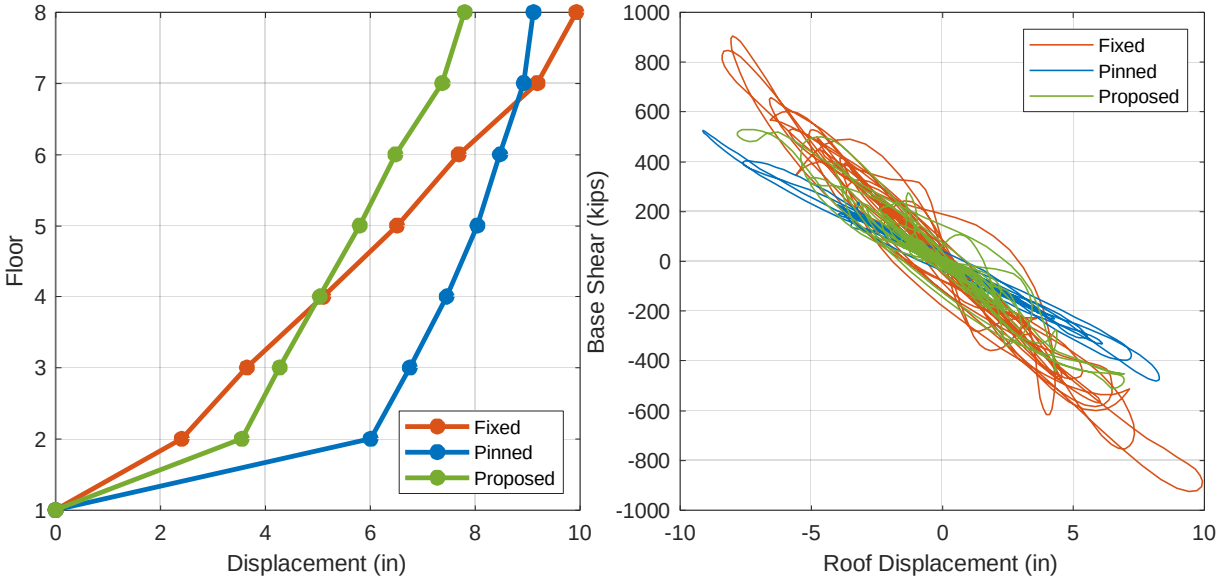

a) b)

Figure 4.8. a) E-W Exterior Frame Maximum Displacements per floor and b) Base Shear vs. Roof Displacement – Northridge

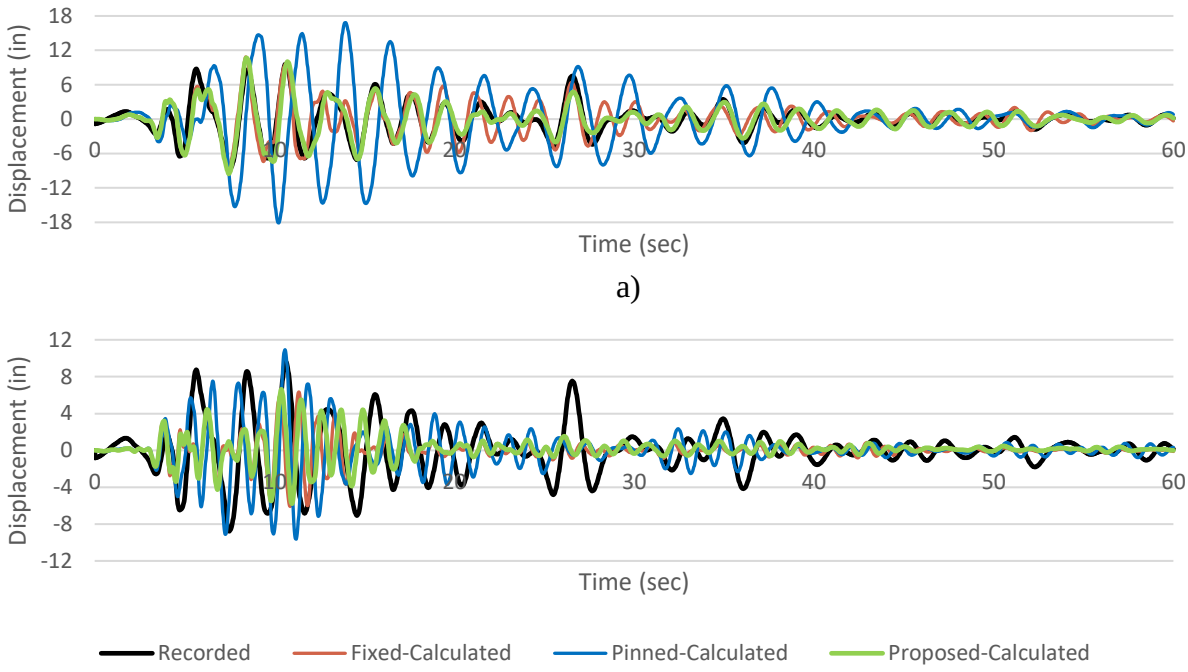

a)

b)

Figure 4.9. a) Roof Displacement Time History for N-S Interior Frame – Northridge and b) N-S Exterior Frame – Northridge

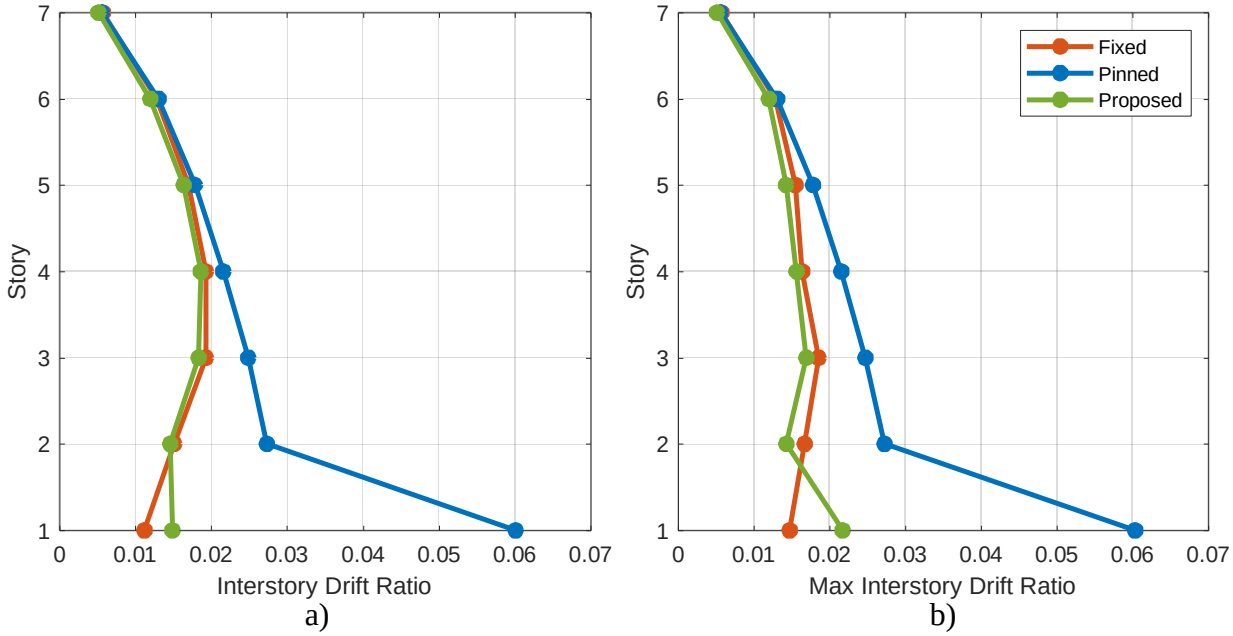

Figure 4.10. a) N-S Interior Frame IDR: Interstory Drift Ratio (IDR) at max roof displacement, and b) Max IDR: the maximum interstory drift ratio for each story – Northridge

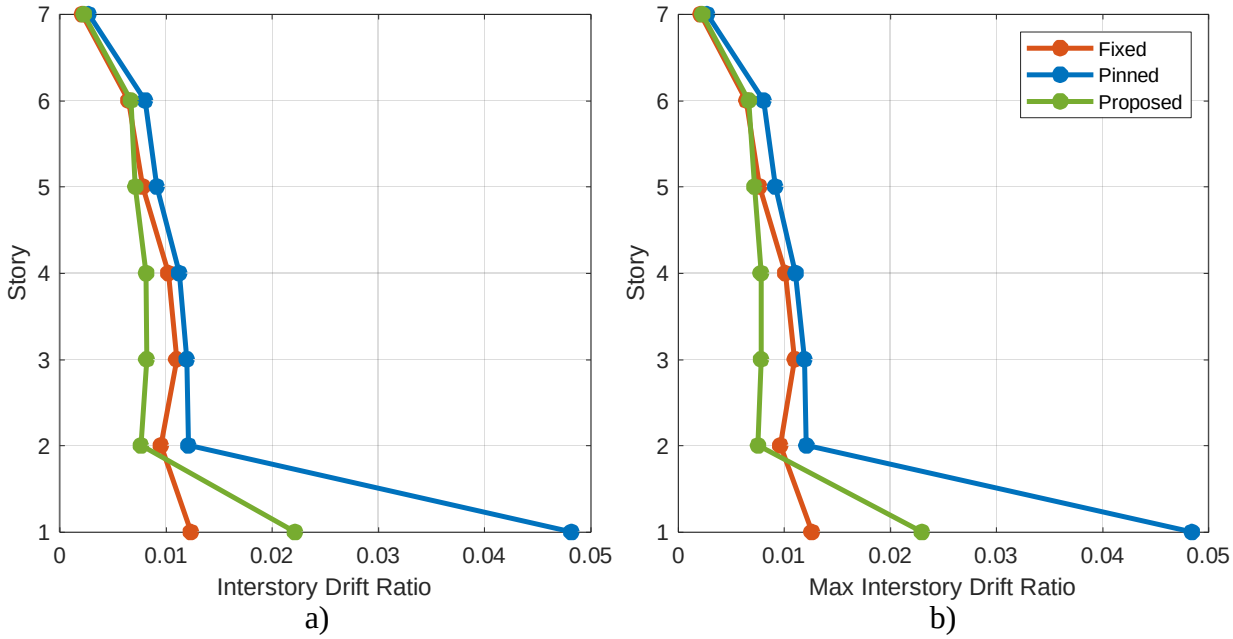

Figure 4.11. a) N-S Exterior Frame IDR: Interstory Drift Ratio (IDR) at max roof displacement, and b) Max IDR: the maximum interstory drift ratio for each story – Northridge

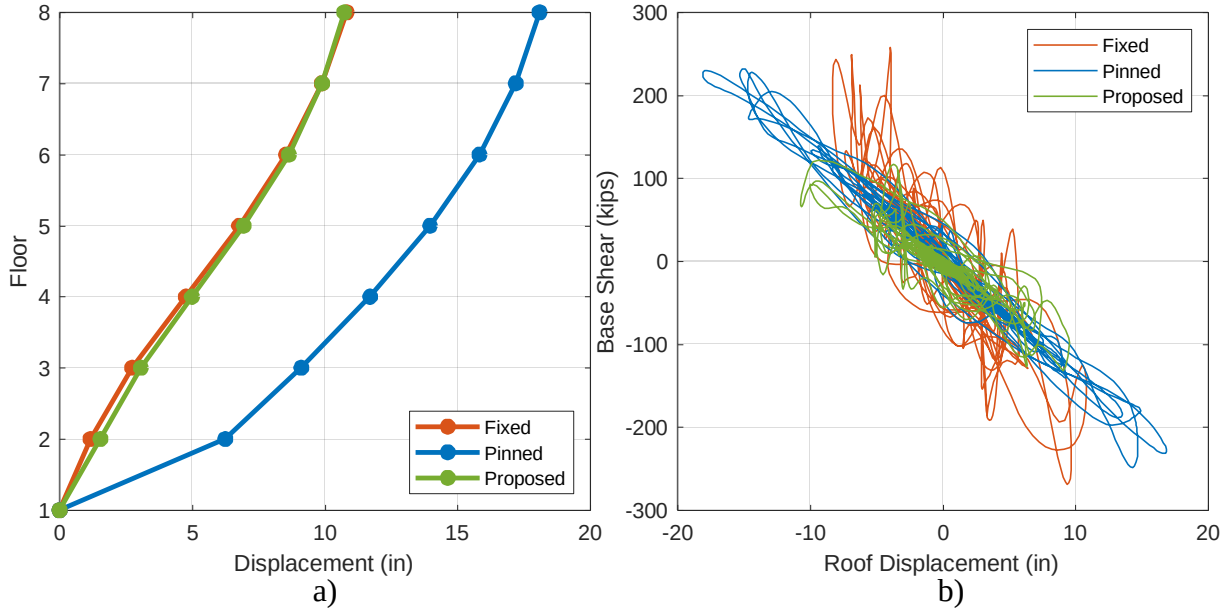

Figure 4.12. a) N-S Interior Frame Maximum Displacements per floor and b) Base Shear vs. Roof Displacement – Northridge

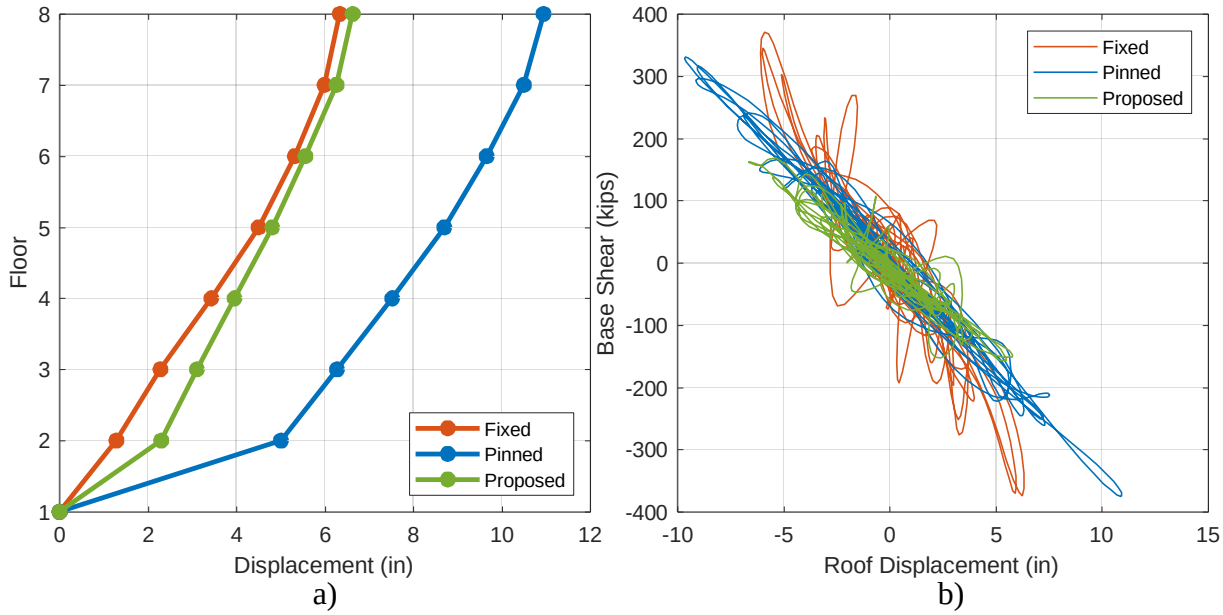

Figure 4.13. a) N-S Exterior Frame Maximum Displacements per floor and b) Base Shear vs. Roof Displacement – Northridge

4.5 1992 Landers Earthquake Ground Motion

The Landers earthquake has a duration of 80 seconds. The results in Figure 4.14 and Figure 4.19 display both fixed and pinned overestimating or underestimating the displacement values, where the proposed rotational spring follows closely to the fixed base condition. The exterior frame observes similar observation for E-W and N-S frames and potential reasoning are described later. The results from Figure 4.15-Figure 4.16 and Figure 4.20-Figure 4.21 show the difference in behavior between pinned, fixed, and proposed rotational spring models. The proposed rotational spring interstory drift ratio values, for the most part, follows closely to the fixed base condition. In the first story, the IDR for pinned is about three times that of fixed, with proposed rotational spring in between. Whereas the estimated values in the first story using the fixed assumption are around 30% less than those obtained using the proposed rotational spring for the interior frame, and around 45% less in the exterior frames. In the N-S direction, the estimated values in the first story using the fixed assumption are 25% less than those obtained using the proposed rotational spring for the interior frame, and around 30% less in the exterior frame, both of which are smaller differences than in the E-W frame. The results from Figure 4.17-Figure 4.18 and Figure 4.22-Figure 4.23 show the maximum displacement always located at the roof, but the behavior of the intermediate floors change shape according to the response. The base shear decreases as base condition goes from fixed to proposed to pinned. Contrary, the N-S exterior frame displays the pinned base condition with the greatest base shear and roof displacement, but is explained with the behavior response difference to that of fixed displaying a max roof displacement 60% less than those obtained in the pinned base, greatest between all frames for Landers.

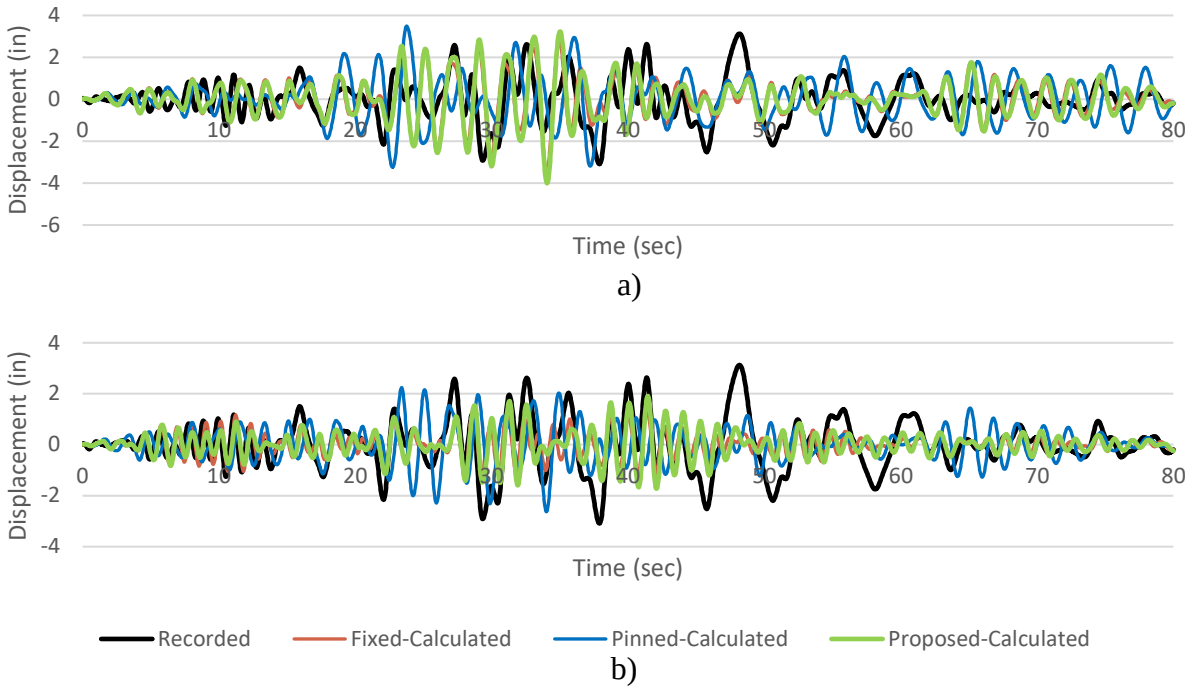

Figure 4.14. a) Roof Displacement Time History for E-W Interior Frame – Landers and b) E-W Exterior Frame – Landers

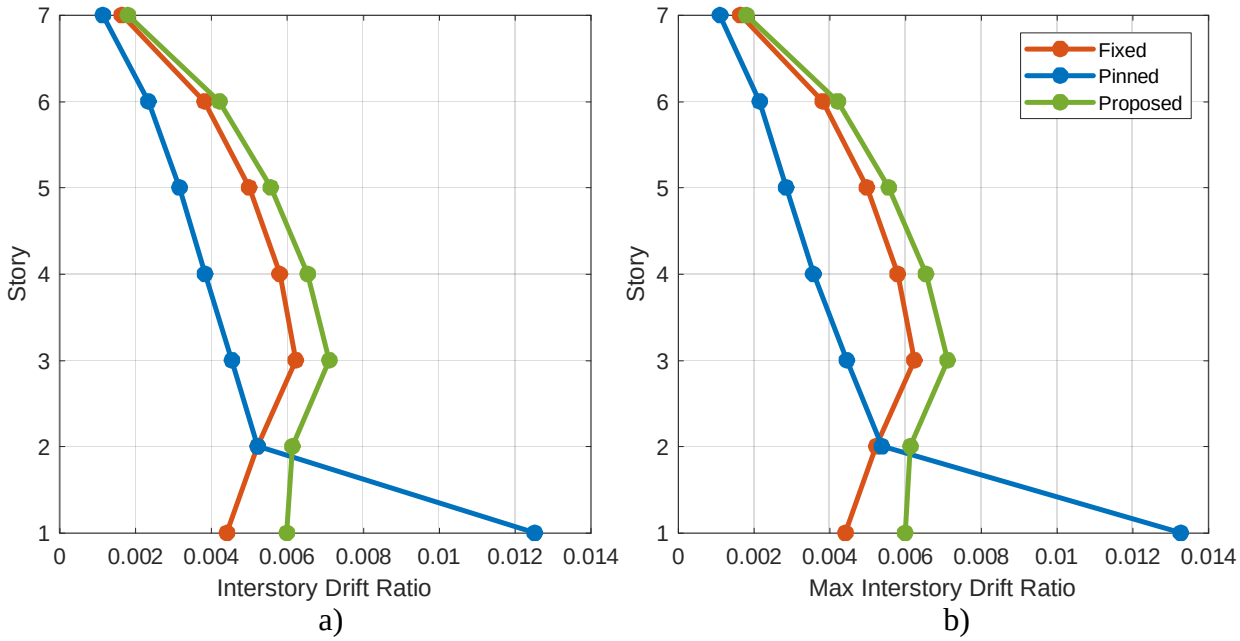

Figure 4.15. a) E-W Interior Frame IDR: Interstory Drift Ratio (IDR) at max roof displacement, and b) Max IDR: the maximum interstory drift ratio for each story – Landers

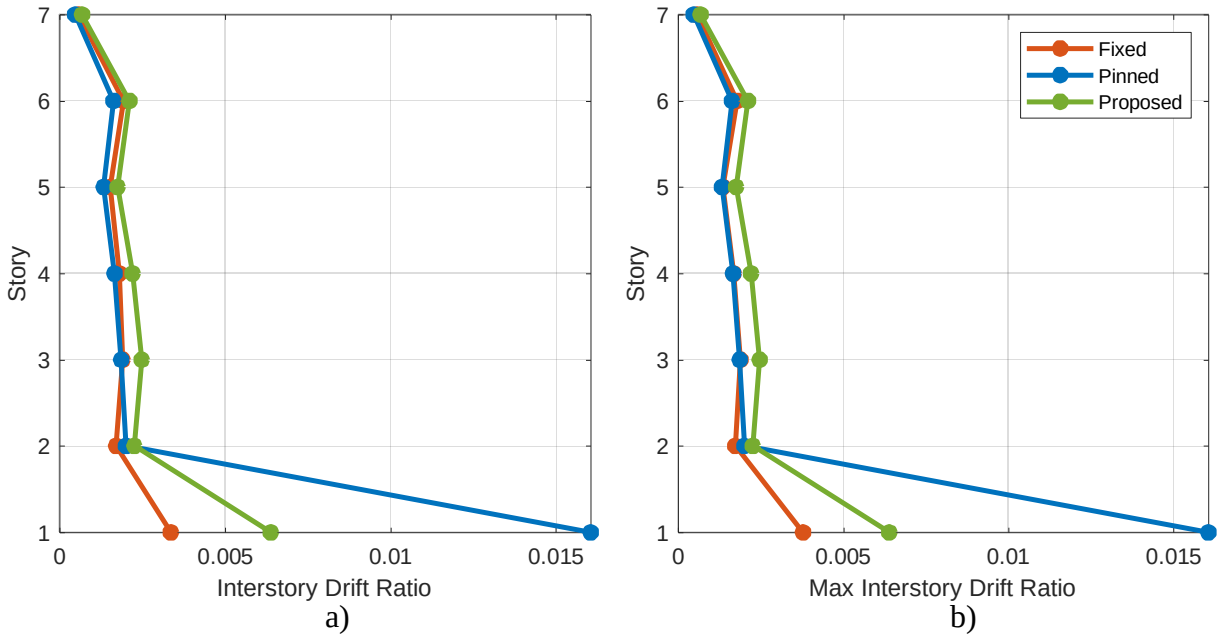

Figure 4.16. a) E-W Exterior Frame IDR: Interstory Drift Ratio (IDR) at max roof displacement, and b) Max IDR: the maximum interstory drift ratio for each story – Landers

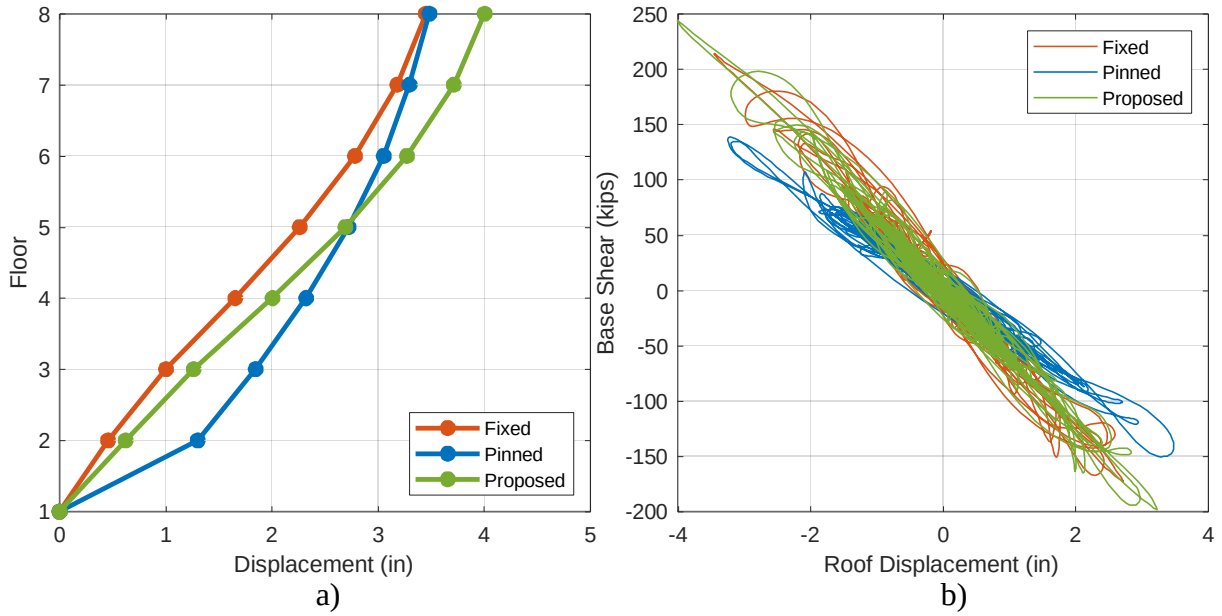

Figure 4.17. a) E-W Interior Frame Maximum Displacements per floor and b) Base Shear vs. Roof Displacement – Landers

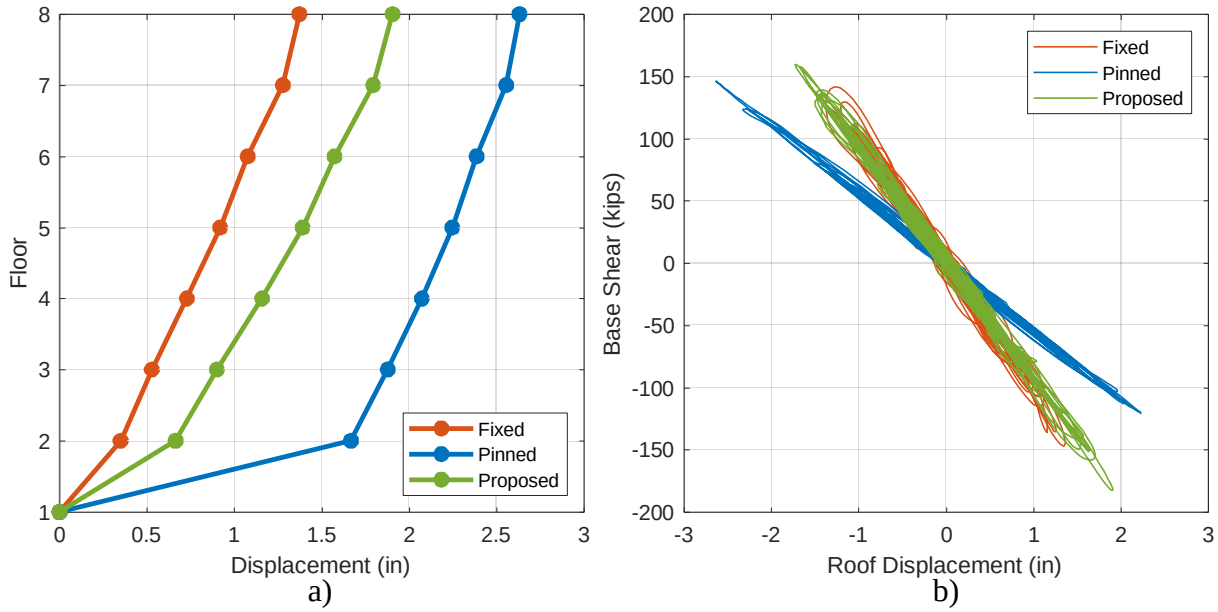

Figure 4.18. a) E-W Exterior Frame Maximum Displacements per floor and b) Base Shear vs. Roof Displacement – Landers

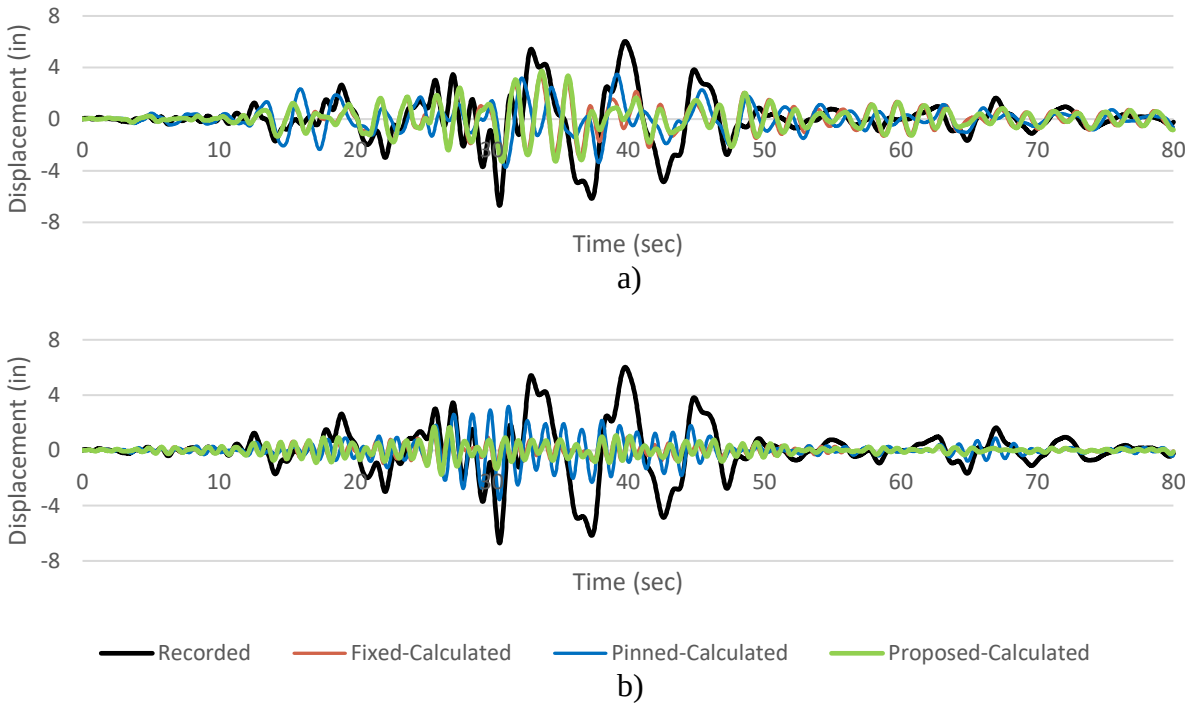

Figure 4.19. a) Roof Displacement Time History for N-S Interior Frame – Landers and b) N-S Exterior Frame – Landers

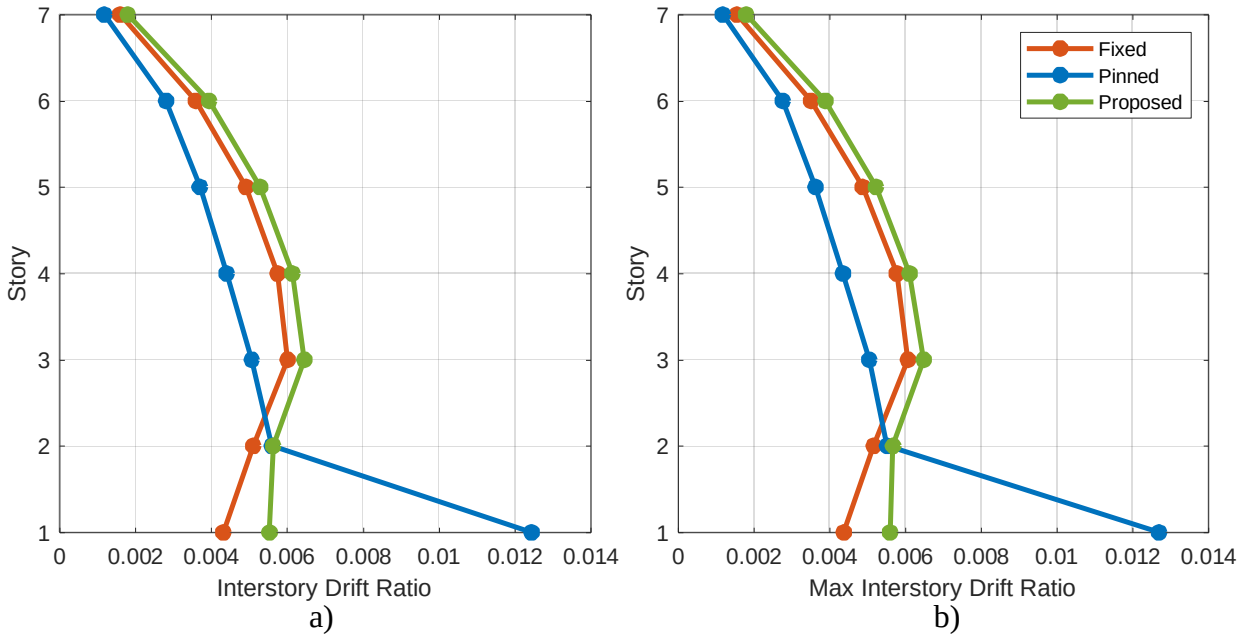

Figure 4.20. a) N-S Interior Frame IDR: Interstory Drift Ratio (IDR) at max roof displacement, and b) Max IDR: the maximum interstory drift ratio for each story – Landers

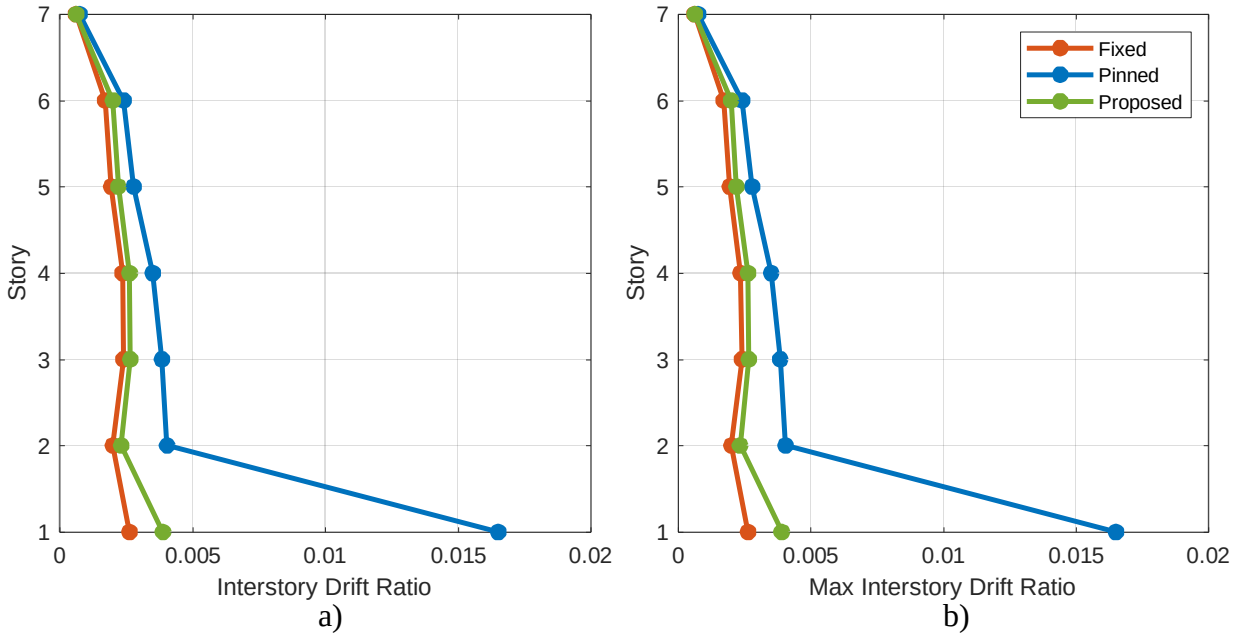

Figure 4.21. a) N-S Exterior Frame IDR: Interstory Drift Ratio (IDR) at max roof displacement, and b) Max IDR: the maximum interstory drift ratio for each story – Landers

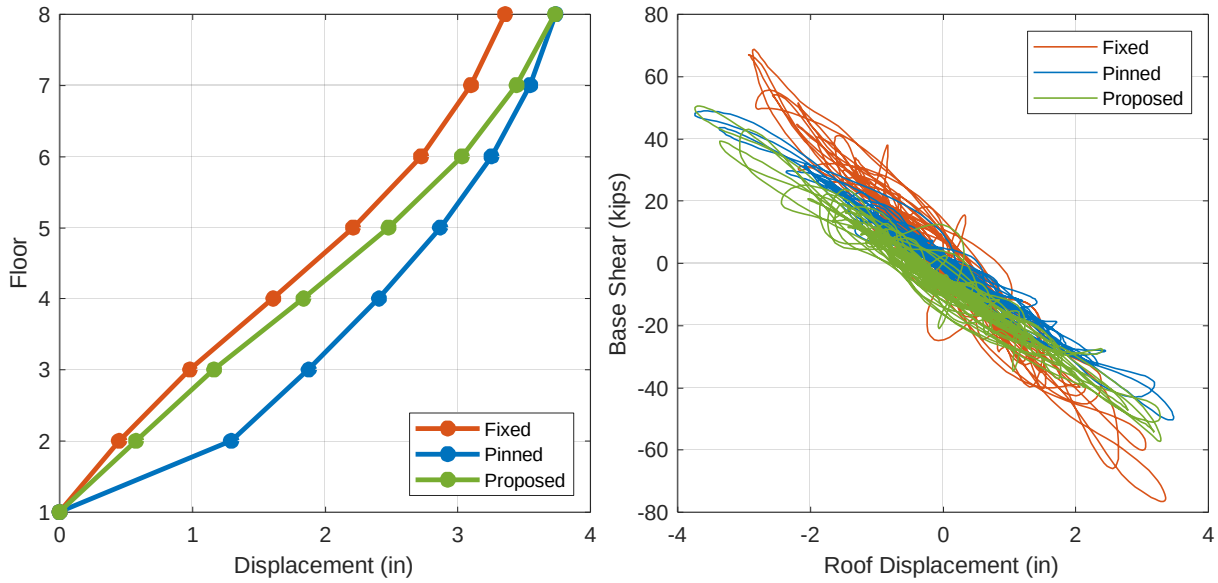

a) b)

Figure 4.22. a) N-S Interior Frame Maximum Displacements per floor and b) Base Shear vs. Roof Displacement – Landers

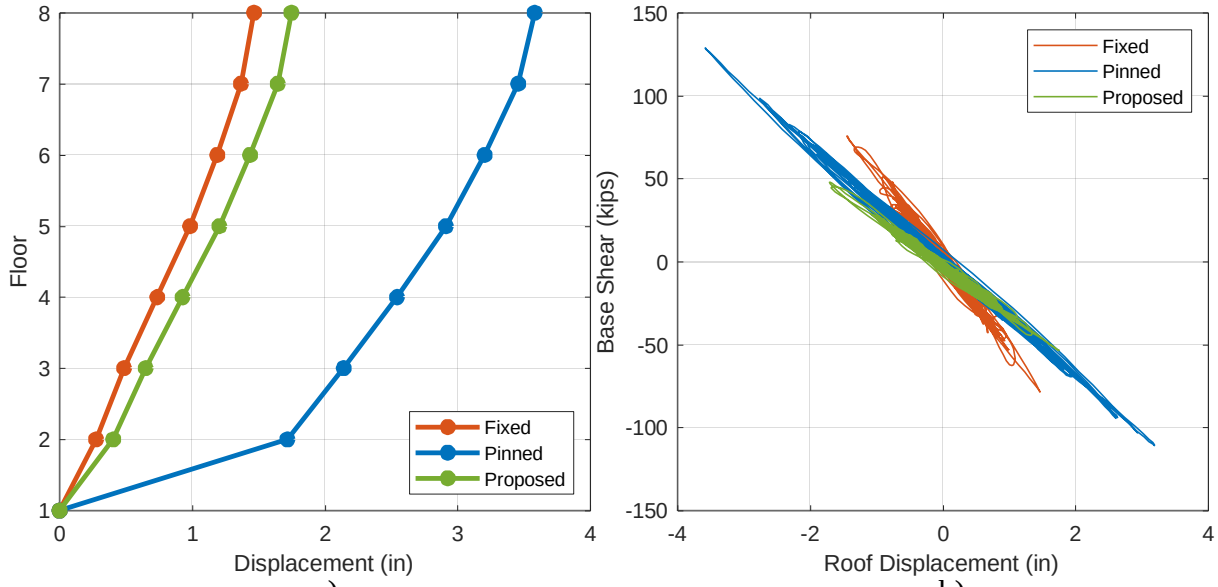

a) b)

Figure 4.23. a) N-S Exterior Frame Maximum Displacements per floor and b) Base Shear vs. Roof Displacement – Landers

4.6 1971 San Fernando Earthquake Ground Motion

The San Fernando earthquake has a duration of about 60 seconds. The results in Figure 4.24 and Figure 4.29 display both fixed and pinned overestimating or underestimating the displacement

values, where the proposed rotational spring follows closely to the fixed base condition. The exterior frame observes similar observation for E-W and N-S frames and potential reasoning are described later. The results from Figure 4.25-Figure 4.26 and Figure 4.30-Figure 4.31 show the difference in behavior between pinned, fixed, and proposed rotational spring models. The proposed rotational spring interstory drift ratio values, for the most part is close to those values of the fixed base condition. In the first story, the IDR for pinned is about three to four times that of fixed, with proposed rotational spring in between. Whereas the estimated values in the first story using the fixed assumption are around 35% to 45% less than those obtained using the proposed rotational spring for the interior frame, and around 45% less in the exterior frames. In the N-S direction, the estimated values in the first story using the fixed assumption are 35% to 45% less than those obtained using the proposed rotational spring for the interior frame, and around 35% less in the exterior frame, both of which are similar differences to the E-W frame.. The results from Figure 4.27-Figure 4.28 and Figure 4.32-Figure 4.33 show the maximum displacement always located at the roof, but the behavior of the intermediate floors change shape according to the response. The base shear decreases as base condition goes from fixed to proposed to pinned. Contrary, the E-W interior and N-S exterior frame displays the pinned base condition with the greatest base shear and roof displacement, but is explained with the behavior response difference to that of fixed displaying a max roof displacement 50% to 60% less than those obtained in the pinned base, greatest between all frames for San Fernando.

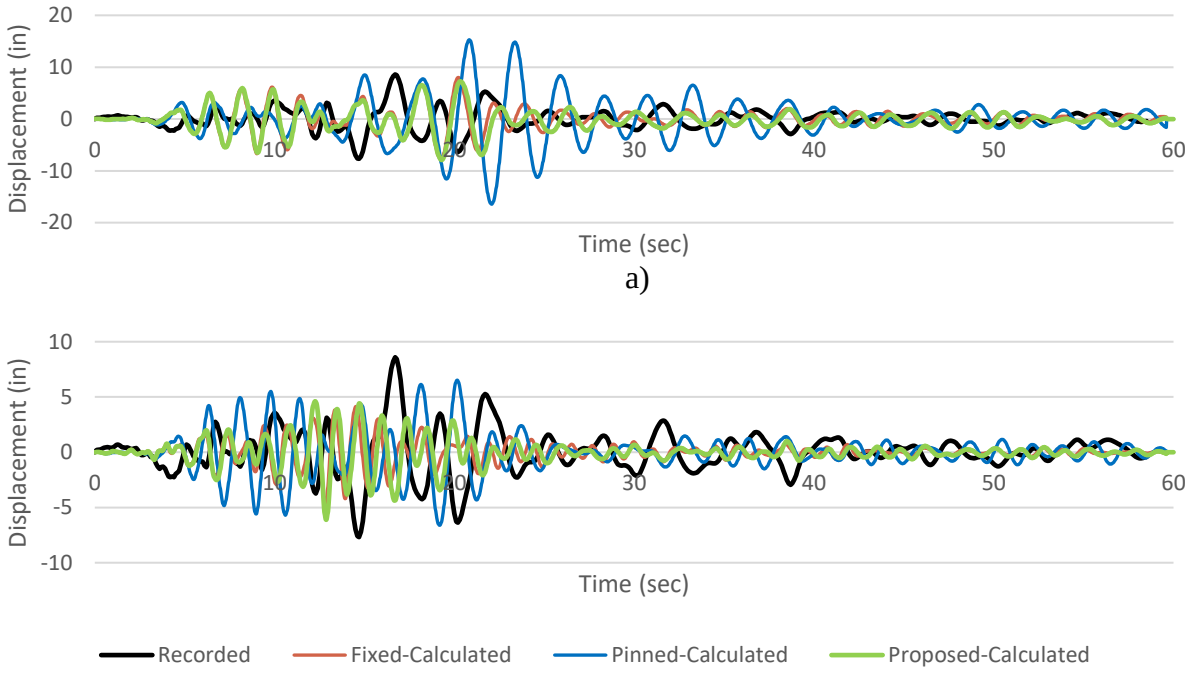

Figure 4.24. a) Roof Displacement Time History for E-W Interior Frame – San Fernando and b) E-W Exterior Frame – San Fernando

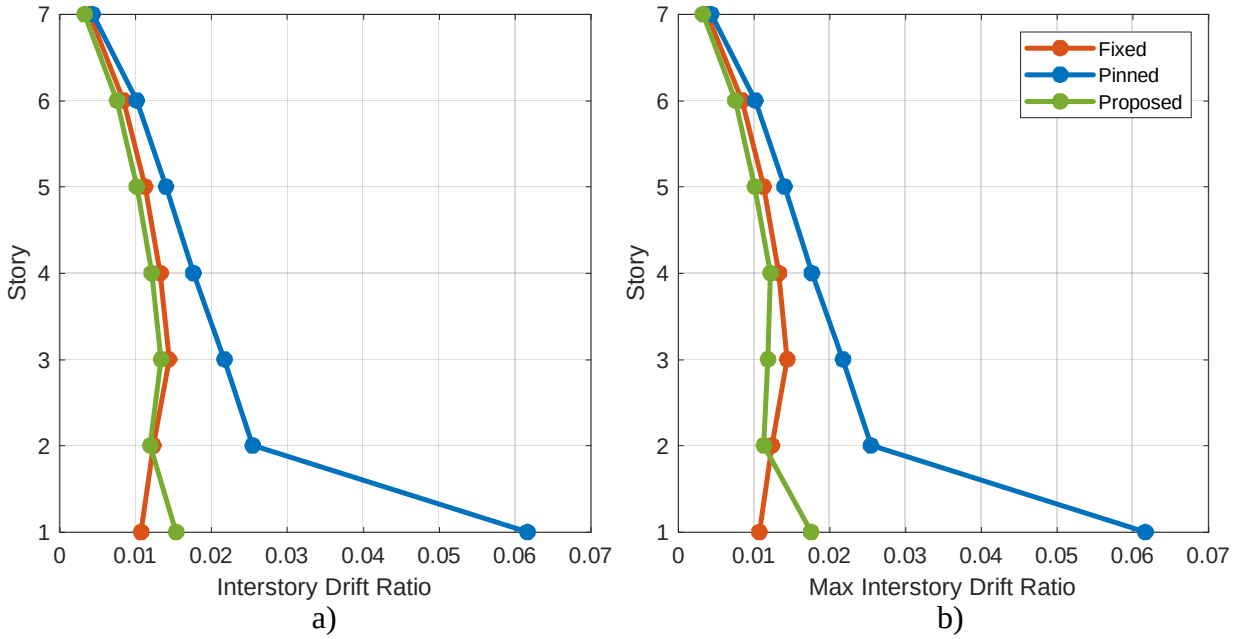

Figure 4.25. a) E-W Interior Frame IDR: Interstory Drift Ratio (IDR) at max roof displacement, and b) Max IDR: the maximum interstory drift ratio for each story – San Fernando

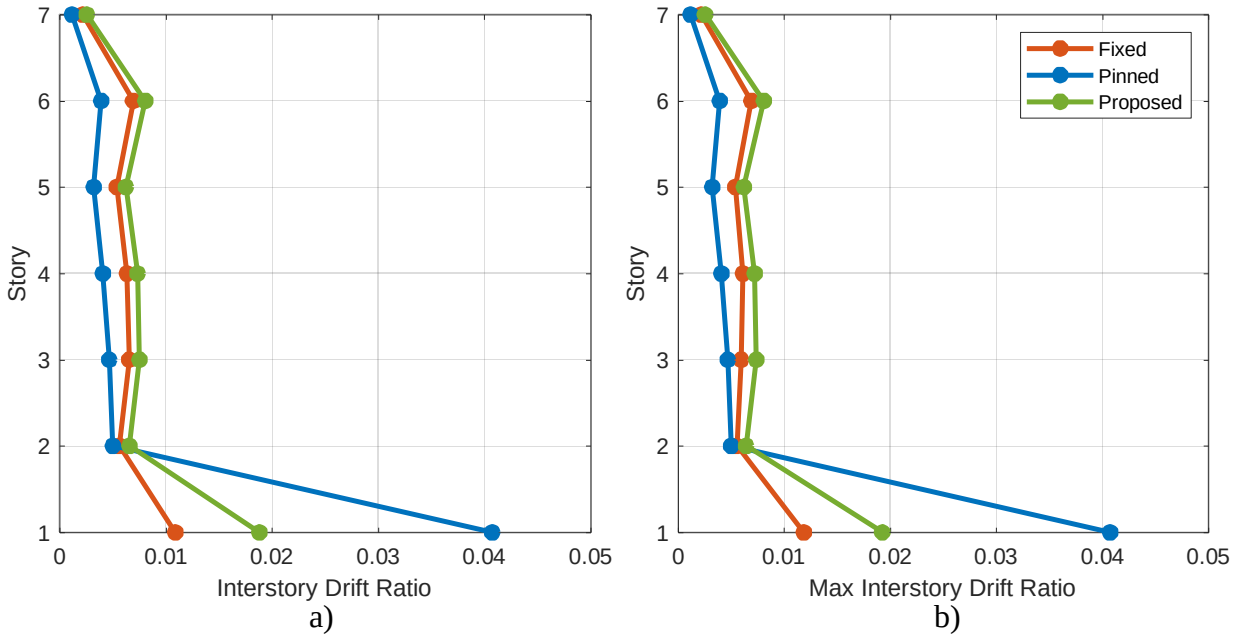

Figure 4.26. a) E-W Exterior Frame IDR: Interstory Drift Ratio (IDR) at max roof displacement, and b) Max IDR: the maximum interstory drift ratio for each story – San Fernando

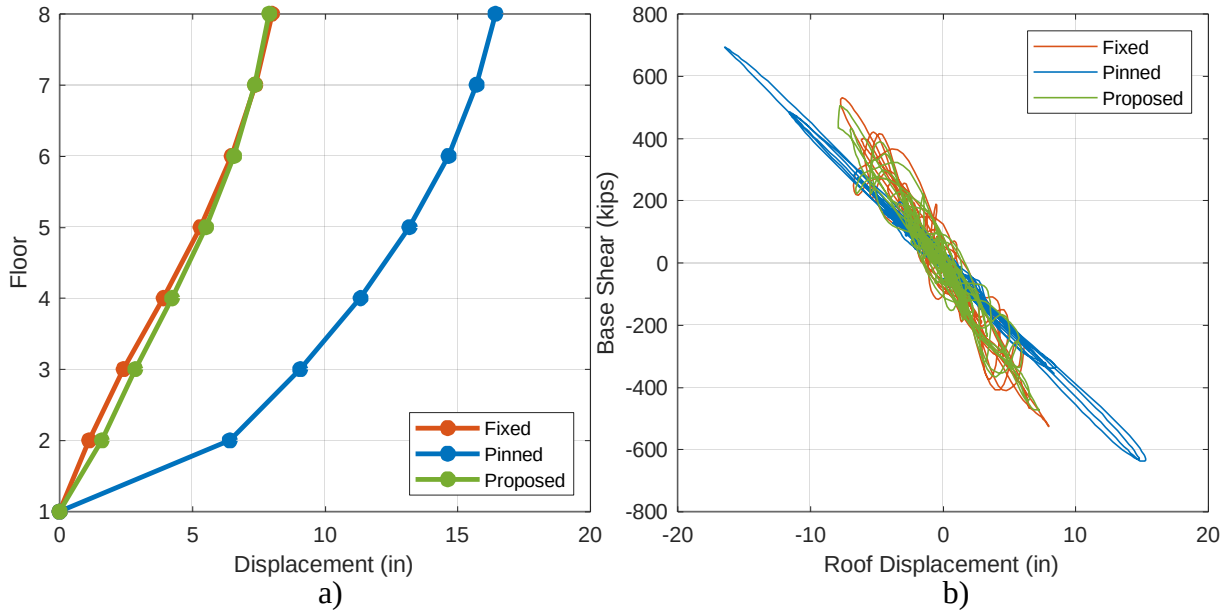

Figure 4.27. a) E-W Interior Frame Maximum Displacements per floor and b) Base Shear vs. Roof Displacement – San Fernando

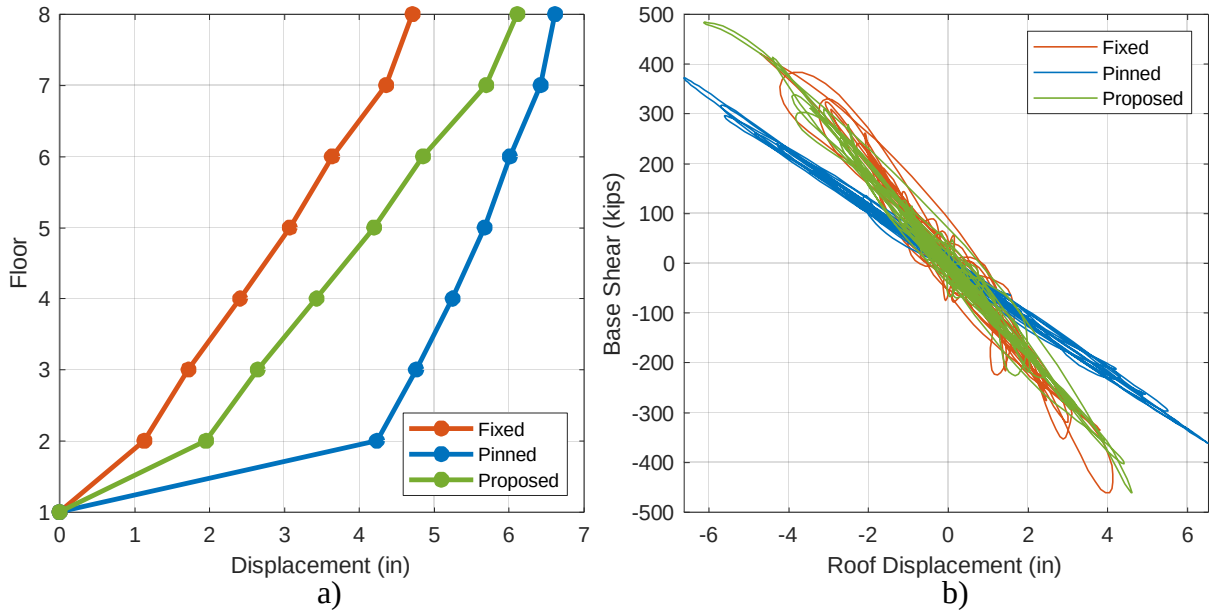

Figure 4.28. a) E-W Exterior Frame Maximum Displacements per floor and b) Base Shear vs. Roof Displacement – San Fernando

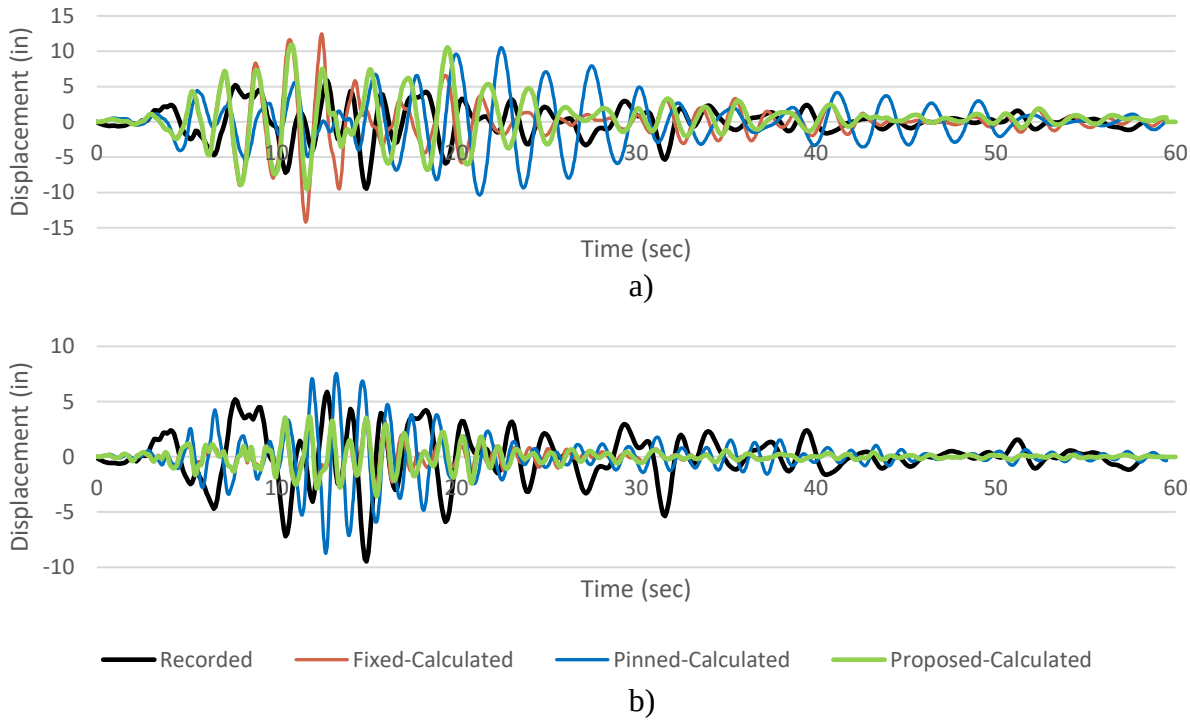

Figure 4.29. a) Roof Displacement Time History for N-S Interior Frame – San Fernando and b) N-S Exterior Frame – San Fernando

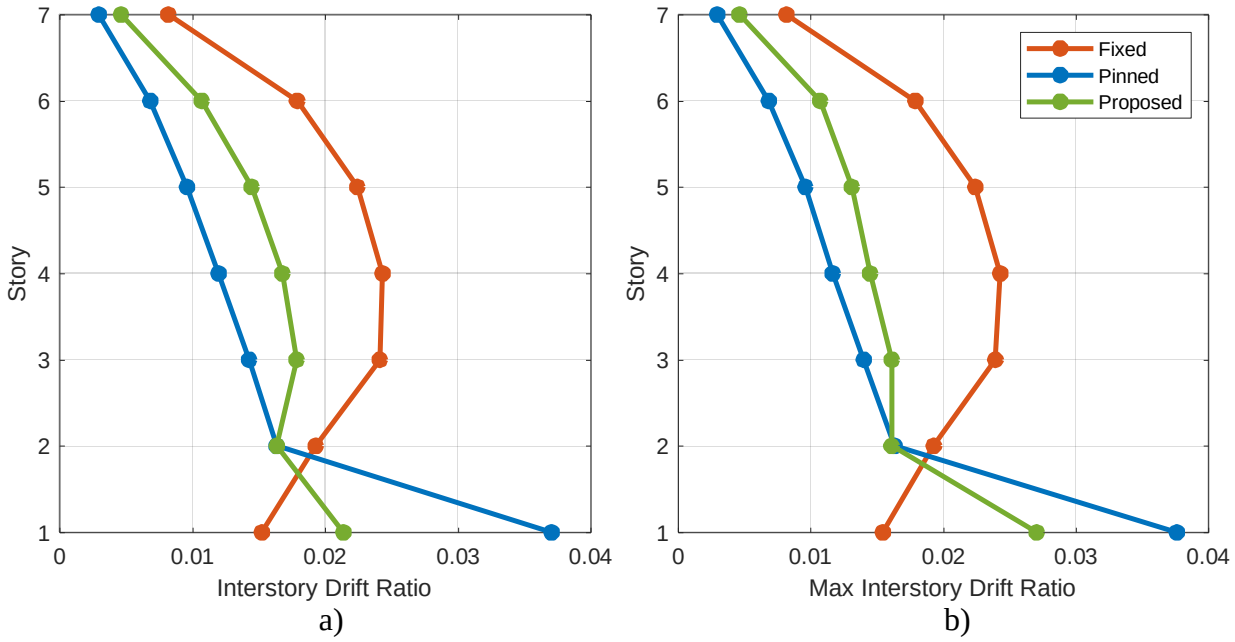

Figure 4.30. a) N-S Interior Frame IDR: Interstory Drift Ratio (IDR) at max roof displacement, and b) Max IDR: the maximum interstory drift ratio for each story – San Fernando

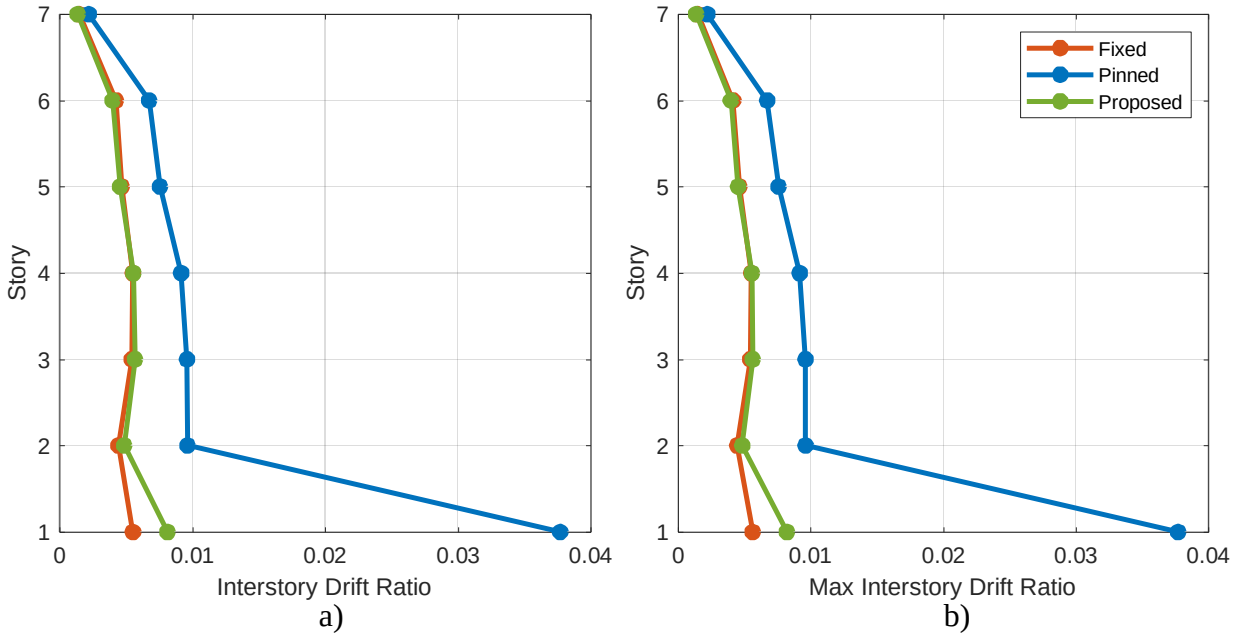

Figure 4.31. a) N-S Exterior Frame IDR: Interstory Drift Ratio (IDR) at max roof displacement, and b) Max IDR: the maximum interstory drift ratio for each story – San Fernando

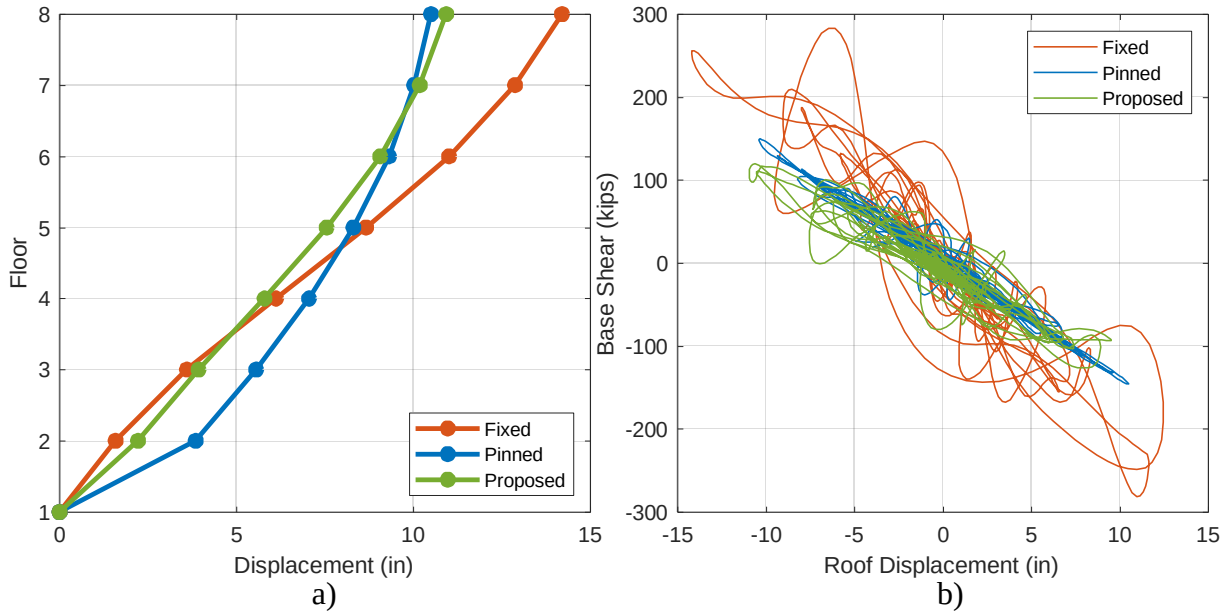

Figure 4.32. a) N-S Interior Frame Maximum Displacements per floor and b) Base Shear vs. Roof Displacement – San Fernando

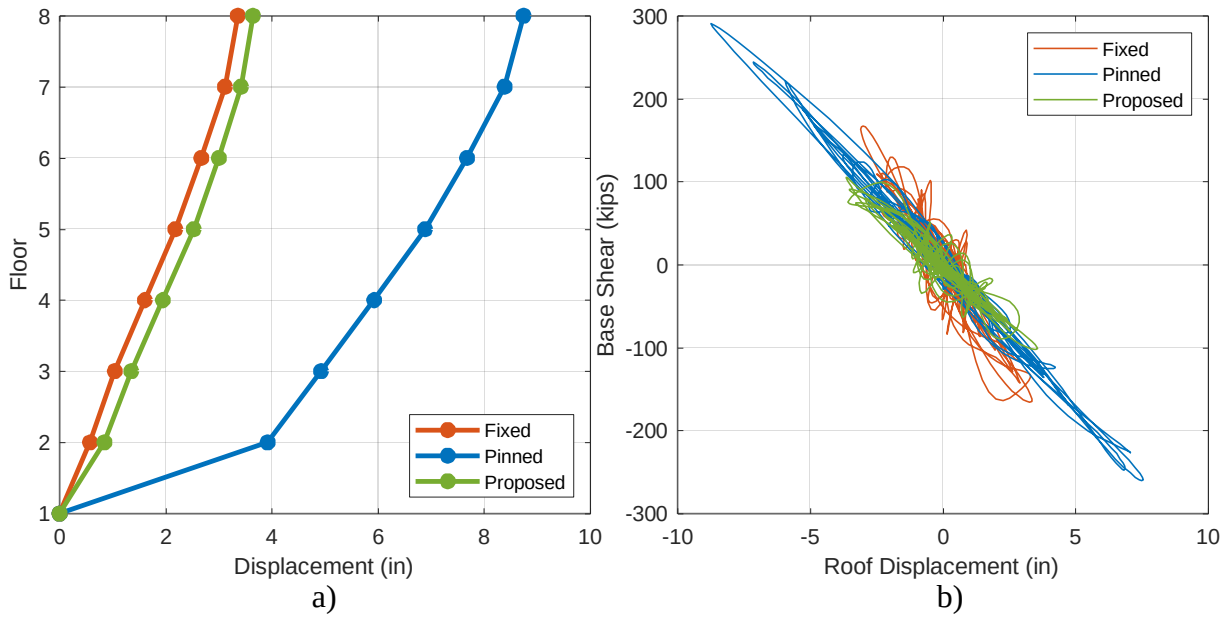

Figure 4.33. a) N-S Exterior Frame Maximum Displacements per floor and b) Base Shear vs. Roof Displacement – San Fernando

4.7 1987 Whittier Earthquake Ground Motion

The Whittier earthquake has a duration of 40 seconds. The results in Figure 4.34 display both fixed and pinned overestimating or underestimating the displacement values, where the

proposed rotational spring follows closely to the fixed base condition. The exterior frame observes similar observation for the pinned condition, whereas the proposed rotational spring obtains a better agreement to the recorded values for the N-S frame. Potential reasoning is described later. The results from Figure 4.35 and Figure 4.36 show the difference in behavior between pinned, fixed, and proposed rotational spring models. The proposed rotational spring interstory drift ratio values, for the most part, follows closely to the fixed base condition. In the first story, the IDR for pinned is about twice times that of fixed, with proposed rotational spring in between. Whereas the estimated values in the first story using the fixed assumption are around 15% to 25% less than those obtained using the proposed rotational spring for the interior frame, and around 25% less in the exterior frames. The results from Figure 4.37 and Figure 4.38 show the maximum displacement always located at the roof, but the behavior of the intermediate floors change shape according to the response. The base shear decreases as base condition goes from fixed to proposed to pinned.

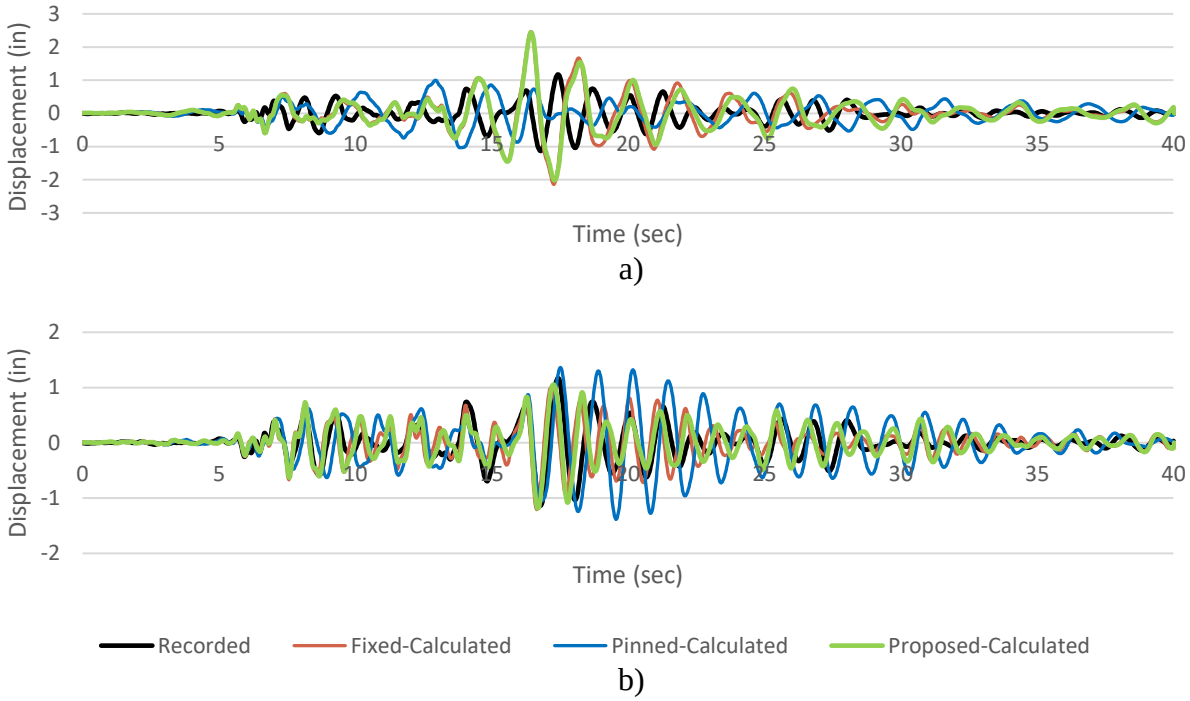

Figure 4.34. a) Roof Displacement Time History for N-S Interior Frame – Whittier and b) N-S Exterior Frame – Whittier

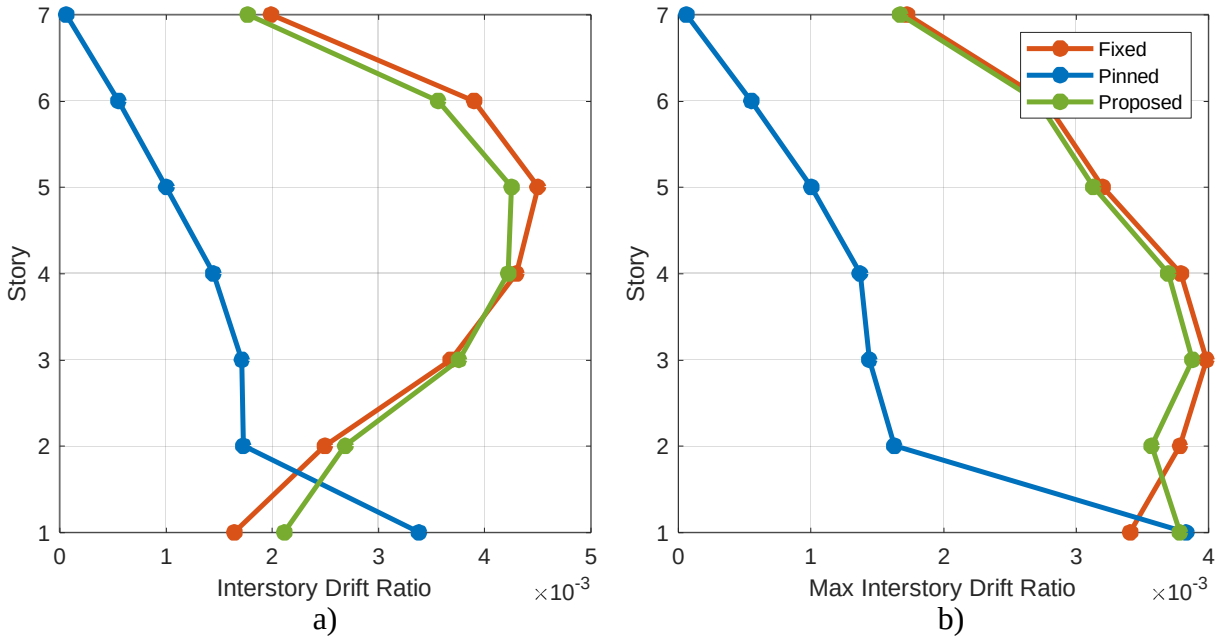

Figure 4.35. a) N-S Interior Frame IDR: Interstory Drift Ratio (IDR) at max roof displacement, and b) Max IDR: the maximum interstory drift ratio for each story – Whittier

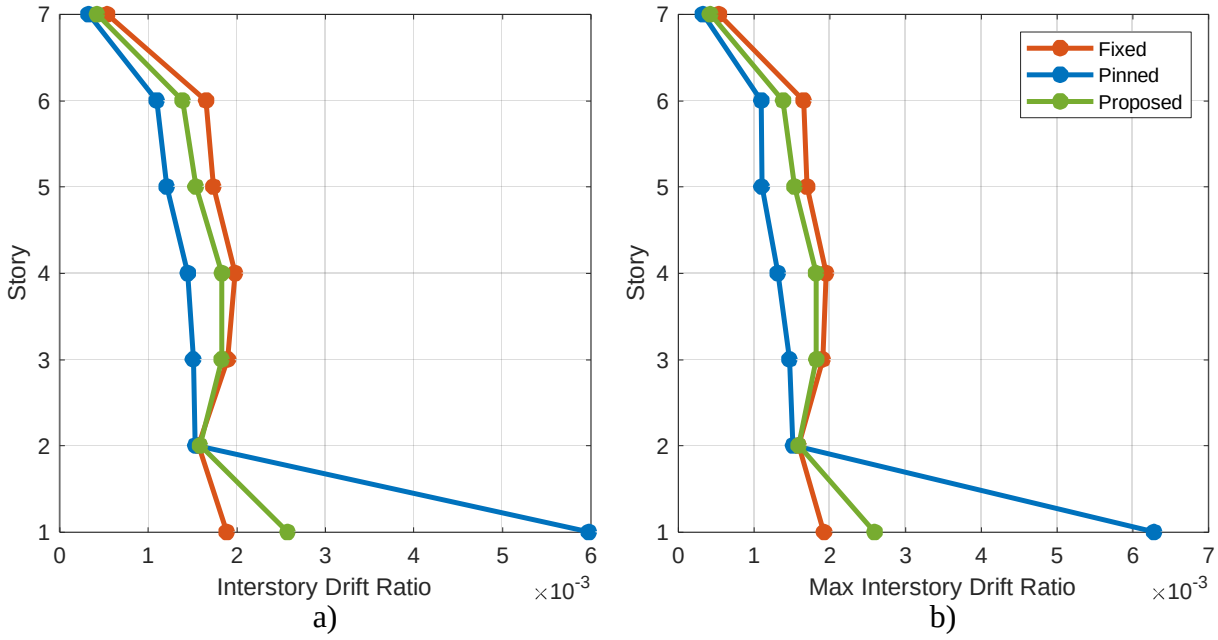

Figure 4.36. a) N-S Exterior Frame IDR: Interstory Drift Ratio (IDR) at max roof displacement, and b) Max IDR: the maximum interstory drift ratio for each story – Whittier

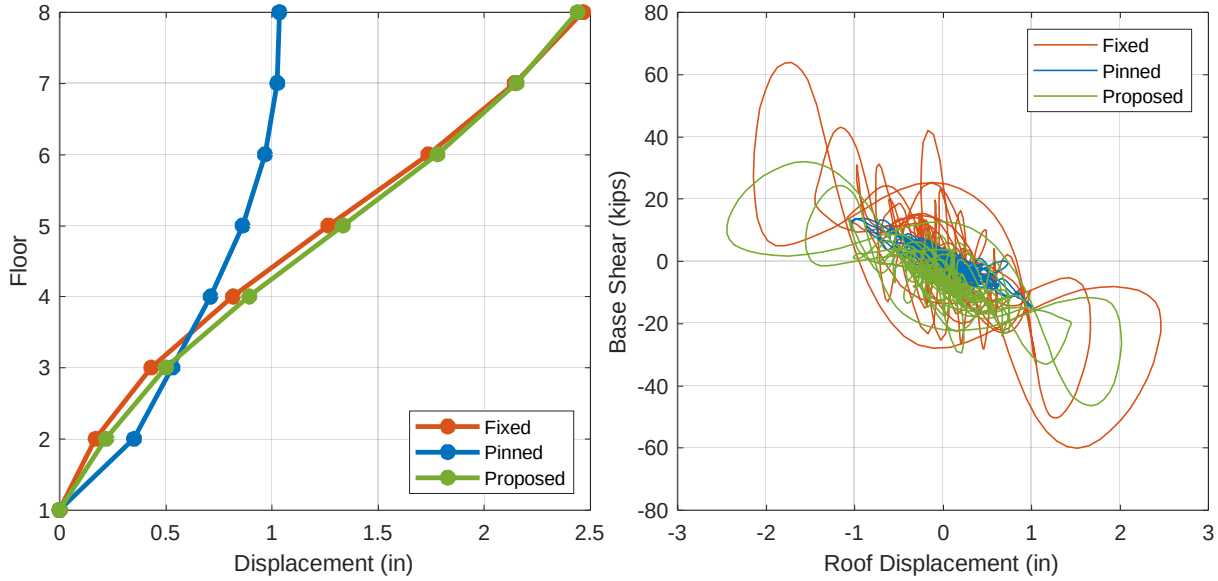

a) b)

Figure 4.37. a) N-S Interior Frame Maximum Displacements per floor and b) Base Shear vs. Roof Displacement – Whittier

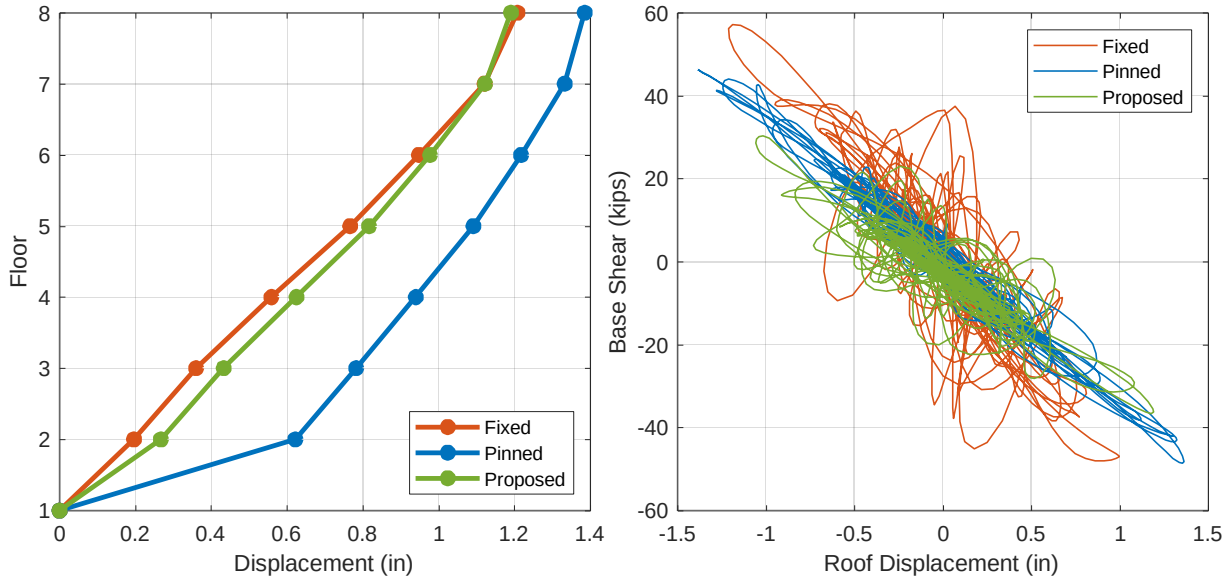

a) b)

Figure 4.38. a) N-S Exterior Frame Maximum Displacements per floor and b) Base Shear vs. Roof Displacement – Whittier

4.8 Summary of Observations

4.8.1 Drift

In Sections 4.4, 4.5, 4.6 and 4.7, some observations were similar among the different earthquakes. In regard to the roof displacement time histories, only the Northridge interior frames E-W and N-S and Whittier Exterior N-S had good agreement to the recorded performance of the building. These results are influenced by the building period, the type of earthquake intensity, and potentially other out of scope considerations such as soil-structure interaction. While not occurring at all times in time history, often the fixed and pinned base condition roof displacement values overestimated and underestimated, respectively, when compared to recorded values. From the comparison of the three base conditions alone, a typical observation was that the proposed rotational spring landed between the fixed and pinned values, noticeably closer to the fixed condition and even closer to the recorded value. Without the consideration of a couple of masonry walls present in the first story and other external factors, the values with the proposed short lap splices results in reasonable values when compared to the recorded values.

The interstory drift ratios (IDR) follow similar trends. The max IDR values for proposed rotational spring landed between the fixed and pinned base condition results at all instances for the first story. All the pinned base condition results show the largest interstory drift ratio at the first story, resembling the soft-story mechanism. The interior and exterior frames showed differences in terms of behavior. While typically the maximum displacement occurs at the roof, all the exterior frames, in both directions for the three base conditions, resemble a soft-story mechanism and the critical first mode of vibration behavior. The interior frames for fixed and proposed base condition showed the larger interstory drift ratio occurring in the intermediate floors of the building, resembling a higher mode vibration behavior. This behavior offers an explanation for the shear failures observed in the intermediate stories of Van Nuys building for the Northridge earthquake. The interior and exterior frames showed different behavior due to the dynamic characteristics changing, including influential factors like in inertial forces, mass and stiffness, and the limitations of a two-dimensional analysis. In general, the observations showed the effects of adding some restraint. In the interior frames, once the restraint and modeling of the splice is implemented compared to pinned, the behavior changes and potentially soft story no longer is seen as an issue, and rather intermediate stories can be vulnerable, depending on the ground motion. The lap splice

lengths were also different between interior columns of $24d_b$ and exterior columns of $36d_b$. Table 4.2 presents the difference of maximum interstory drift ratio in the first story for both between fixed to proposed and pinned to proposed. At all instances, the proposed base condition was closer to the fixed base condition max IDR values, except N-S Whittier interior frame. For N-S direction, the proposed base condition max IDR value was closer to the pinned base condition for the interior frame versus exterior frame. For E-W direction, the proposed base condition max IDR value was closer to the pinned base condition for the exterior frame in comparison to interior frame. The difference between observations for the orthogonal directions possibly mostly due to frame characteristics rather than the lap splice length, in which were not considered a substantial change.

Table 4.2. Difference of Maximum Interstory Drift Ratios in First Story

	N-S Interior		N-S Exterior		E-W Interior		E-W Exterior	
	Fixed-Prop.	Pinned-Prop.	Fixed-Prop.	Pinned-Prop.	Fixed-Prop.	Pinned-Prop.	Fixed-Prop.	Pinned-Prop.
Northridge	0.00697	0.03864	0.01039	0.02546	0.00534	0.01381	0.01467	0.01917
Landers	0.00122	0.00710	0.00126	0.01261	0.00158	0.00728	0.00260	0.00966
San Fernando	0.01159	0.01060	0.00258	0.02950	0.00680	0.04414	0.00741	0.02147
Whittier	0.00037	0.00005	0.00067	0.00369				

4.8.2 Force Demand

Observations between the base conditions in terms of forces are valuable to understand the demands on the structure and its behavior with respects to force. Generally speaking, forces in both flexure and shear are highest when the base is fixed. One of the potential reasoning for modeling a frame or building with a fixed base is because it is the case with the highest forces. Once rotation is allowed, forces are reduced and displacements are typically increased. Contrary to the statement, three frames display the pinned base condition with the greatest base shear and roof displacement, but is explained with the behavior response difference to fixed base condition showing the greatest difference compared to the rest of the frames in terms of maximum roof drift and first story inter story drift ratio. More importantly is the comparison between the fixed and proposed base conditions, where the addition of the rotational spring results in shear and forces decreasing. Drift and forces are both important when considering a dynamic analysis, and due to other external factors, drift is an important indicator for building behavior specifically in seismic

events. Shear forces were checked for the critical forces found in the fixed base condition, see Section 3.8. While for the Northridge earthquake a few columns in the intermediate stories failed in shear, demand was less for the other base conditions and remaining earthquakes in the case study building. Shear strength forces were typically adequate, and hence shear deformations were considered negligible compared to flexure and slip deformations. In the exterior frames, it was observed that moment demands were greater than the yield moments. This effect of the flexure deformation also helps explain the difference in behavior between exterior and interior frames for a given ground motion. The base shear also indicated that shear demand decreases when base condition goes from fixed to pinned, and displacement decreases. Where the reinforcement yields, the behavior allows the greatest displacement at the roof when pinned, correlating with the maximum interstory drift ratio occurring in the first floor. While Northridge did experience shear failure at a couple of beam-column joints, the amount of damage recorded were only a few columns in the middle floors and possibly not affecting the global building behavior as seen through the good agreement of displacement values, especially earlier in the time history with the shear failure occurring at a later time. While shear failures are important, they did not affect the global building behavior as much comparatively to flexure and slip deformations.

5. SUMMARY AND CONCLUSIONS

5.1 Study Objective and Methodology

The objective of this study was to explore the effects on the behavior when modeling of the base condition incorporates the performance of lap splices which are shorter than modern code requirements. This is a detail often found in older reinforced concrete buildings. Short lap splices were modeled as a rotational spring calibrated to Harajli & Mabsout (2002) bond – stress vs slip relationship. Confidence in the procedure was generated from reproducing the moment – rotation results presented by Cho & Pincheira (2004) for a column specimen. A case study building with short lap splices at the base was located in Van Nuys, California is used to evaluate the inclusion of the shorter lap splices in the modeling. The building is a seven-story perimeter frame NDCB instrumented since the 1971 San Fernando earthquake. The building was modeled in both orthogonal directions using typical two dimensional exterior and interior frames.

The frames were assembled with information from as-built drawings. The model used a lumped plasticity model approach. Observations from the application of a fixed and pinned base connection established the boundary limits of the behavior of the building. Existing literature recommended the use of a bond-stress vs slip relationship and moment – curvature sectional analysis to establish a rotational spring to model the short lap splice. Properties of the rotational spring were calibrated for each frame, namely the moment – rotation curve, and applied to the models.

The finite element software SAP2000 was used to compute the dynamic response of the case study building. The model considered nonlinearity aspects. Several assumptions were applied that provides some limitations of the study. The potential limitations are later explained.

5.2 Observations and Conclusions

The following are the observations and conclusions from this study:

1. **Drift:** The performance of the three base conditions was evaluated by comparing roof drift, interstory drift, and base shear estimates. With respect to drift, the proposed base condition predicted a response in between fixed and pinned

conditions. The proposed rotational spring led to the difference in behavior. The difference between pinned and fixed was apparent in all aspects, especially in the internal frames due to the member elements behavior. When comparing against recorded values, other factors were found to influence the calculated responses, hence while the rest of the frames weren't well predicted in terms of values, the trends observed follow closely to the objective of this study to compare the behavior of the three base conditions.

2. **Interstory Drift:** The ratios showed that the values obtained with the short splice model were between fixed and pinned conditions, especially for the first story. The pinned base conditions and exterior frames all resembled the behavior of soft-story mechanism or a first mode of vibration behavior. Explanations for this type of behavior include the model characteristics, such as mass and stiffness, and also behavior of the elements to the applied forces where moments indicate yielding of the longitudinal bars. The interior frames for fixed and proposed base conditions displayed having the greatest interstory drift ratio in the intermediate floors of the building. A fixed base condition does not allow any rotation or displacements, meanwhile a pinned connection allows free rotation. The proposed rotational spring allows rotation to a certain extent that is based on the relationships of the short lap splice bond stress – slip and moment – curvature sectional analysis. The pinned behavior is shown to display soft story behavior. The proposed rotational spring considers the short lap splice and therefore limits the rotation, where the behavior changes and potentially soft story no longer is seen as an issue and rather intermediate stories can be vulnerable, depending on the ground motion. The lap splice lengths were also different between interior columns of $24d_b$ and exterior columns of $36d_b$, both considered below modern code requirements and observed similar calculated behavior in Table 4.2. In the range of lap splice length considered in this study, short lap splice behavior is expected. However, this study should not be extrapolated to all lengths of short lap splices less than code required because in the assumptions involved in the development of bond-stress vs slip behavior that has built-in parameter assumptions based on type of bar and type of concrete.

3. **Base Shear:** The forces decreased as base condition changed from fixed to proposed to pinned. Once rotation is allowed, forces are reduced, but displacements increased. Shear strength forces were typically adequate, depending on the ground motion, and hence shear deformations were considered negligible compared to flexure and slip deformations. Base shear comparisons show that after rotation is allowed, forces are visibly reduced and displacements are typically increased. This observation holds true for results of fixed and proposed base connections. Pinned base connection sometimes have the highest base shear in comparison, but this difference is due to a higher difference in behavior and essentially overestimation of displacement due to soft story effect. Pinned behavior provides a boundary limit and comparison capability, but realistically the behavior of a short lap splice is closer to that of fixed base, as shown throughout this study. In the exterior frames, it was observed moment demands exceeded calculated yield moments. Longitudinal reinforcement yielding changed the behavior of the frames, as seen through in the exterior frames and all pinned base connections. While under the Northridge ground motion the building did experience shear failure at a couple of beam-column joints, the amount of damage recorded was limited to only a few columns in the 3rd, 4th and 5th floors and produced local damage. Shear failure observed in Northridge was not included in the model. Base shear provided a good illustration of how the shear forces change with different base conditions. Assumptions deemed acceptable for the objective of this thesis and type of columns, include steel reinforcement only considered elastic, perfectly plastic and slap-column joints considered rigid. Although potentially influential parameters were excluded, the results displays reasonable patterns for the calculated roof displacements, interstory drift ratios, and base shear, and demonstrating short lap splice change the drift and displacement values, i.e. the behavior of a non-ductile reinforced concrete case study building.

5.3 Future Work

The following topics are suggested for future research efforts:

1. Several assumptions such as beam-column joints at upper floors and shear deformation springs, while small in comparison to other factors, are recommended for a better simulation.
2. The bond stress vs. slip relationship used was validated with experimental results, but experimental tests with short lap splices subjected to cyclic loading are still considered limited. Tests would improve the understanding of the behavior of short lap splices.
3. Soil-foundation interaction or soil-structure interaction were assumed to be negligible for this study. Exploring the influence of these factors for NDCB frames could improve the simulation of earthquake response.
4. The case study frame was a perimeter frame building. While it is considered more vulnerable compared to other framing systems, modeling of other types of frames can help understand the behavior since NDCB definition are inclusive of other framing systems.
5. The models were two-dimensional and limited the building response. It is envisioned that in some specific cases 3-D models could improve estimation of the response.

APPENDIX A.

Lap Splice Model Calibration Procedure & Results

The Van Nuys building had two different two lap splice lengths, $24d_b$ for interior columns and $36d_b$ for exterior columns. As described in Section 4.2, the considered short lap splice lengths were modeled through the application of local bond stress vs slip and moment – curvature sectional analysis relationship. With those two relationships, the moment – rotation is calculated, then applied and defined in SAP2000 as the property in a nonlinear multilinear plastic type link. The following display the results for a typical interior and a typical exterior column. The first story columns are named C-35 (exterior) and C-26 (interior) from Table 2.1.

Figure A.1 show the local bond stress – slip relationship calculated using Harajli & Mabsout's (2002) model, following the curve for unconfined concrete which relates to a splitting failure. Certain parameter values recommended by Harajli & Mabsout were used due to insufficient data on the bars, such as for S1, S2, and S3. The local bond stress – slip relationship does not change between interior and exterior column because the required inputs are equal. Figure A.2 shows the Force vs Slip at the end of the bar calculated as described in Section 4.2. Figure A.3 display the moment curvature analysis values that are being activated for calculating the moment – rotation relationship. The overall moment – curvature plot was obtained through SAP2000 sectional analysis with the input of the section properties and the axial load acting on that first story column, also obtained through the SAP2000 model. Figure A.4 display the moment – rotation relationships for each column, as they were input in SAP2000. Refer to Harajli & Mabsout (2002) and Cho & Pincheira (2004) for additional details.

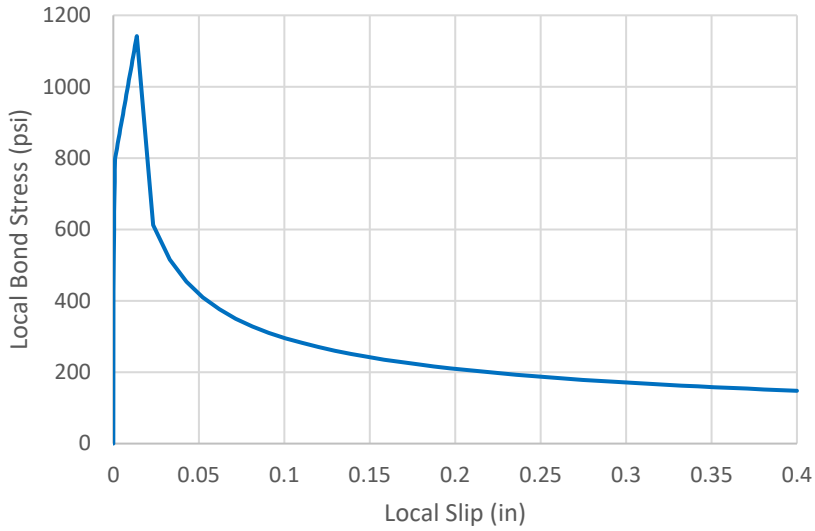

Figure A.1. Local Bond Stress vs Local Slip

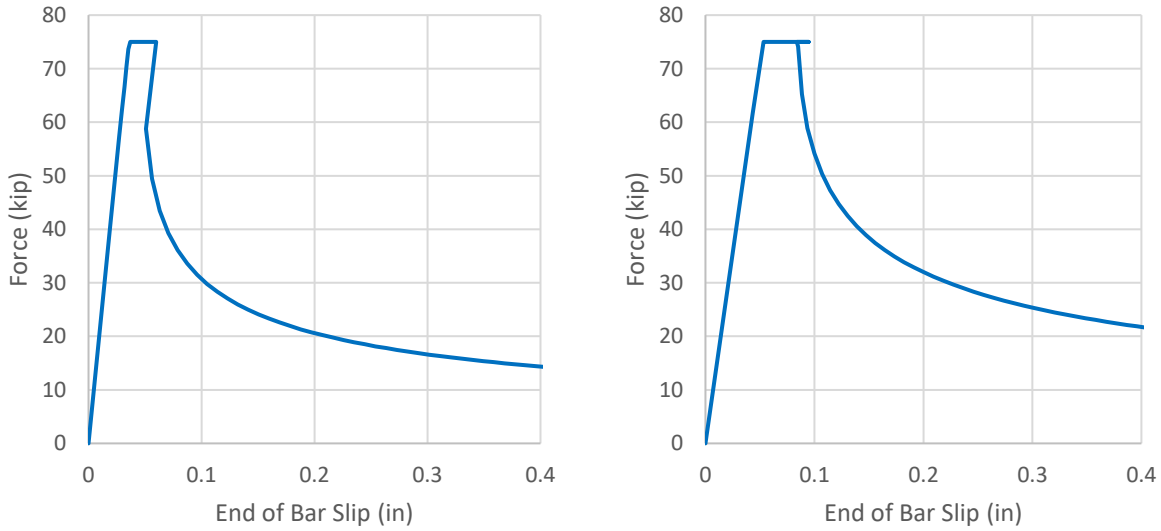

Figure A.2. a) Interior Col. Force vs. End Slip and b) Exterior Col. Force vs. End Slip

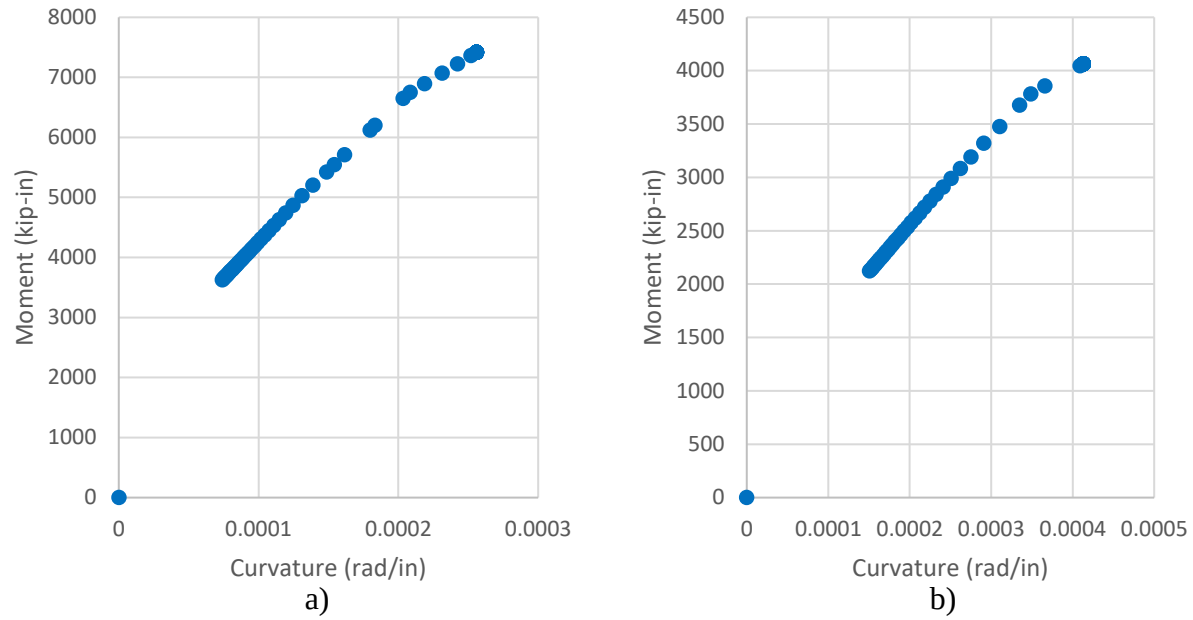

a) b)

Figure A.3. a) Interior Col. and b) Exterior Col. Moment vs. Curvature Values Utilized

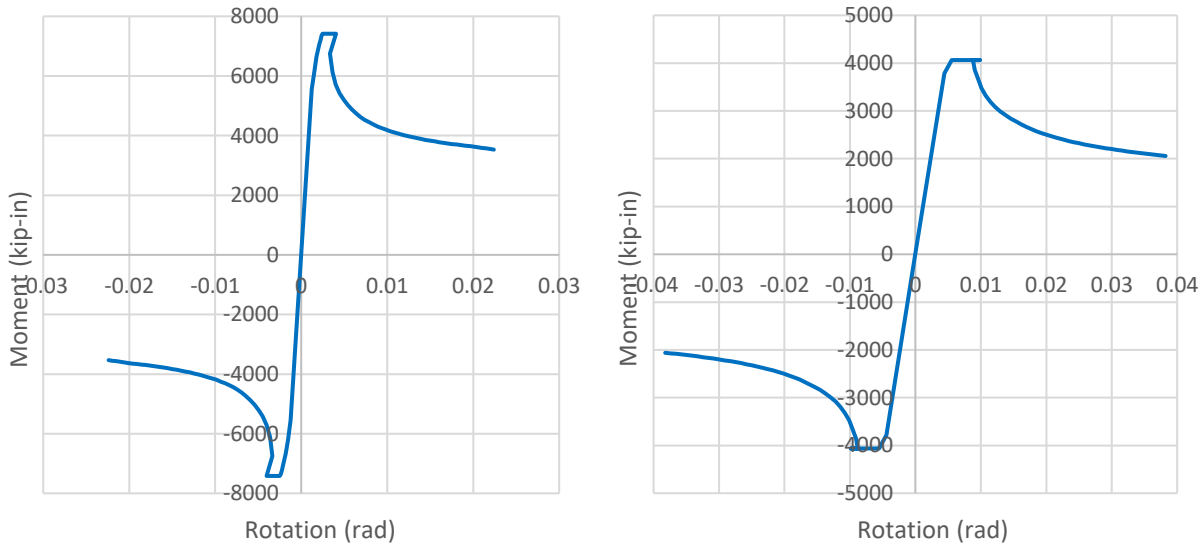

a) b)

Figure A.4. a) Interior Col. and b) Exterior Col. Moment vs. Rotation

REFERENCES

Aboutaha, R. S. (1994). *Seismic retrofit of non-ductile reinforced concrete columns using rectangular steel jackets* (Doctoral dissertation, The University of Texas at Austin). Retrieved from ProQuest Dissertations & Theses Global (Order No. 9519235)

ASCE 41. (2017). *Seismic Evaluation and Retrofit of Existing Buildings* (ASCE/SEI 41-17). American Society of Civil Engineers. https://doi.org/10.1061/9780784414859

Baradaran Shoraka, M., Yang, T. Y., & Elwood, K. J. (2013). Seismic loss estimation of non-ductile reinforced concrete buildings. *Earthquake Engineering & Structural Dynamics*, *42*(2), 297–310. https://doi.org/10.1002/eqe.2213

Barin, B., & Pincheira, J. A. (2002). *Influence of Modeling Parameters and Assumptions on the Seismic Response of an Existing RC Buildings*.

Blume, J. A. (1973). *Holiday Inn, San Fernando, California, Earthquake of February 9, 1971*. U.S. Department of Commerce, National Oceanic and Atmospheric Administration (NOAA), Washington, D.C.

Center for Engineering Strong Motion Data [CESMD]. (n.d.). Retrieved December 10, 2019, from https://strongmotioncenter.org/

Cho, J. Y., & Pincheira, J. A. (2006). Inelastic analysis of reinforced concrete columns with short lap splices subjected to reversed cyclic loads. *ACI Structural Journal*, *103*(2), 280–290. https://doi.org/10.14359/15186

Cho, J.-Y., & Pincheira, J. A. (2004). Nonlinear modeling of RC columns with short lap splices. *In 13 WCEE: 13 Th World Conference on Earthquake Engineering Conference Proceedings*.

Chowdhury, S. R., & Orakcal, K. (2012). An analytical model for reinforced concrete columns with lap splices. *Engineering Structures*, *43*, 180–193. https://doi.org/10.1016/j.engstruct.2012.05.019

Computers and Structures Inc. (2008). *SAP2000 Technical Note, Material Stress-Strain Curves*.

Eligehausen, R., Popov, E. P. P., & Bertero, V. V. (1983). *Local Bond Stress-Slip Relationships of Deformed Bars under Generalized Excitations.* UCB/ EERC-83-23.

FEMA. (2018). *FEMA P-2018, Seismic Evaluation of Older Concrete Buildings for Collapse Potential*. www.ATCouncil.org

Holmes, W. T. (2014). Identification and mitigation of collapse prone concrete buildings (ATC 78). *In NCEE 2014 - 10th U.S. National Conference on Earthquake Engineering: Frontiers of Earthquake Engineering*. Earthquake Engineering Research Institute. https://doi.org/10.4231/D3QR4NR2F

Islam, M. S. (1996). Analysis of the Northridge earthquake response of a damaged non-ductile concrete frame building. *The Structural Design of Tall Buildings*, *5*(3), 151–182.

Jennings, P. C. (1971). *Engineering features of the San Fernando earthquake of February 9, 1971*.

Los Angeles Department of Building and Safety [LADBS] (2020). *Non-Ductile Concrete Retrofit Program Status Report*. Retrieved April 30, 2020.

Lepage, A. (1997). *A method for drift-control in earthquake-resistant design of RC building structures* (Doctoral dissertation, University of Illinois at Urbana-Champaign). Retrieved from ProQuest Dissertations & Theses Global. (Order No. 9717299)

Liel, A. B. (2008). *Assessing the collapse risk of California's existing reinforced concrete frame structures: Metrics for seismic safety decisions* (Doctoral dissertation, Stanford University). Retrieved from https://search.proquest.com/docview/20995935?accountid=13360. (Accession No. 9115028)

Lynn, A. C. (2001). *Seismic evaluation of existing reinforced concrete building columns* (Doctoral dissertation, University of California, Berkeley). Retrieved from ProQuest Dissertations & Theses Global. (Order No. 3044578)

Melek, M., & Wallace, J. W. (2004). Cyclic Behavior of Columns with Short Lap Splices. *ACI Structural Journal*, *101*(6), 802–811. https://doi.org/10.14359/13455

Mitchell, D., DeVall, R. H., Saatcioglu, M., Simpson, R., Tinawi, R., & Tremblay, R. (1995). Damage to concrete structures due to the 1994 Northridge earthquake. *Canadian Journal of Civil Engineering*, *22*(2), 361–377. https://doi.org/10.1139/l95-047

Moehle, J. (1998). Existing Reinforced Concrete Building Construction: A Review of Practices and Vulnerabilities in California. *SEAONC Fall Seminar*.

Office of Los Angeles Mayor Eric Garcetti. (2014). *Resilience by Design*. https://www.lamayor.org/resilience-design-building-stronger-los-angeles

Paspuleti, C. (2002). *Seismic Analysis of an Older Reinforced Concrete Frame Structure* (Master's Thesis). The University of Washington

Rissman & Rismann Associated Ltd. (1965). *Drawings of Holiday Inn Building*.

Shakal, A. F., & Huang, M. J. (1985). *Standard tape format for CSMIP strong-motion data tapes: California Division of Mines and Geology*.

Sözen, M. A. (2013). Why Should Drift Drive Design For Earthquake Resistance? *In Proceeding the 6th Civil Engineering Conference in Asia Region: Embracing the Future through Sustainability*.

Suwal, A. (2015). *Evaluation of modeling parameters in ASCE 41-13 for the nonlinear static and dynamic analysis of an RC building* (Master's Thesis, The University of Texas at San Antonio). Retrieved from ProQuest Dissertations & Theses Global. (Order No. 1605159).

Suwal, A. (2018). *Performance evaluation of a non-ductile reinforced concrete moment frame building* (Master's Thesis, The University of Texas at San Antonio). Retrieved from ProQuest Dissertations & Theses Global. (Order No. 13421719).

Trifunac, M.D., Ivanovic, S.S. & Todorovska, M. I. (1999). Instrumented 7-Storey Reinforced Concrete Building in Van Nuys, California: Description of Damage from the 1994 Northridge Earthquake and Strong Motion Data, Department of Civil Engineering, *Report No. CE 99-02*, University of Southern California, Los Angeles, California.

USGS. *United States Geological Survey*. www.usgs.gov